COO-1198-1036

CONTRIBUTIONS FROM POINT DEFECTS TO THE ELASTIC CONSTANTS OF COPPER

Lynn Eduard Rehn

Department of Physics and Materials Research Laboratory

University of Illinois, Urbana, Illinois 61801

February 1974

This technical information document is based on a thesis submitted in partial fulfillment of the requirements for the degree of Doctor of Philosophy in Physics in the Graduate College of the University of Illinois, 1974. This research was supported in part by the U. S. Atomic Energy Commission under Contract AT(11-1)-1198 and by the National Science Foundation Grant GH-33634.

DISCLAIMER

CONTRIBUTIONS FROM POINT DEFECTS TO THE ELASTIC CONSTANTS OF COPPER

BY

LYNN EDUARD REHN

B.A., Albion College, 1967
M.S., University of Illinois, 1969

THESIS

Submitted in partial fulfillment of the requirements
for the degree of Doctor of Philosophy in Physics
in the Graduate College of the
University of Illinois at Urbana-Champaign, 1974

Urbana, Illinois

CONTRIBUTIONS FROM POINT DEFECTS TO THE ELASTIC CONSTANTS OF COPPER

Lynn Eduard Rehn, Ph.D.
Department of Physics
University of Illinois at Urbana-Champaign, 1974

The changes introduced in a complete set of independent copper elastic constants (C_{11}, C_{44} and C') by irradiation with thermal neutrons below 4 K have been measured. Simultaneous measurements of attenuation and resistivity were also performed, and the change in attenuation due to the introduction of defects has been determined. The high degree of sensitivity achieved by using a pulse-echo superposition technique permitted a study to be made of the annealing of these effects through most of stage I.

It was found that the contributions at liquid helium temperatures from different stage I defects to a particular elastic constant were not the same, and the magnitude of the effect from a given defect was found to vary among different constants. Significant temperature dependent effects were also observed in all the elastic constants. The results are discussed in terms of four different effects: a small bulk effect; a larger polarization effect, which involves the stress induced internal displacement of certain defects; a thermally activated relaxation process; and a change in the vibrational spectrum of the lattice from the introduction of defect resonance modes. The indication of a small bulk effect is in agreement with the range of reported theoretical estimates. The results obtained at 3.6 K for the recovery of the results during stage I_D are qualitatively in agreement with a calculation by Dederichs of the polarizability of the ⟨100⟩-split interstitial. The relaxation process previously reported by Nielsen and Townsend has been observed, and we have attributed it to the I_C defect. A model of this defect is proposed. No other relaxation of stage I defects has been observed. The

measurements indicate that both the I_D and I_E defects change the temperature dependence of the elastic constants by introducing resonance modes into the vibrational spectrum of the lattice. The frequency obtained from an analysis of stage I_D is believed to be $5 \times 10^{12} \pm 30\%$ Hz, and is in reasonable agreement with the value of approximately 6×10^{12} Hz obtained by Dederichs et al. with a computer simulation of a ⟨100⟩-split interstitial in a copper lattice. The contribution from this effect to the temperature dependence of other physical properties (resistivity, specific heat and thermal expansion) is discussed. The results obtained here are helpful in understanding apparent discrepancies in previously reported measurements of irradiation induced changes in the elastic constants.

ACKNOWLEDGMENTS

The author would like to express his deep-felt appreciation to his advisors, Professor Jon T. Holder and Professor A. V. Granato, for their continued guidance and many helpful ideas throughout the course of this study.

He would also like to thank the personnel at the Solid State Division of Oak Ridge National Laboratory, Oak Ridge, Tennessee, for many fruitful discussions, and for use of the Low Temperature Irradiation Facility. In particular, he is grateful to Ralph Coltman, Charles Klabunde, Jean Redman and Jim Williams for their invaluable assistance in performing the experiments, to Dr. F. W. Young, Jr., for furnishing the copper samples, and to the entire staff for their friendliness and patience during his visit.

He also appreciates a number of discussions with W. Schilling and P. H. Dederichs.

He is indebted to Dr. Ricardo Schwartz for his assistance in developing the chemical polishing technique used in this experiment.

Finally, the support of the United States Atomic Energy Commission, and the National Science Foundation under contract NSF GH 33634 is acknowledged.

TABLE OF CONTENTS

LIST OF FIGURES

LIST OF TABLES

I. INTRODUCTION

The introduction of lattice vacancies and interstitials by irradiation alters many of the physical properties of solids, but the majority of experiments which have attempted to investigate the behavior of these defects have involved only measurements of defect induced changes in the electrical resistivity. Such studies have contributed much to the understanding of defect behavior, and among other things have shown that the damage created by various types of irradiation particles differs primarily in the local arrangements of the vacancies and interstitials as well as demonstrated the existence of four well-defined recovery stages in all but a few of the face-centered cubic metals. Since it is possible for these defects to aggregate as well as annihilate once they become mobile, the nature of the irradiation produced damage is least complex in the first of these stages, stage I, which involves the annealing range from 0 to 60 K. Measurements by Magnuson, Palmer and Koehler[1] indicated substructure in stage I and a more detailed study by Corbett, Smith and Walker[2,3] (CSW) revealed the existence of five substages in this annealing range. The primary features of the recovery model proposed by CSW for stage I have since become very generally accepted. This model attributes the first three of the sub-stages (I_A, I_B and I_C) to the collapse of vacancy-interstitial close-pairs, the fourth (I_D) to the correlated recombinations of interstitials with their mother vacancies, and the dose-dependent fifth sub-stage (I_E) to the long range migration of an interstitial defect.

Another physical property which can also be conveniently measured with high precision is a change in the stress-strain relationship of a material, represented by its various elastic constants. More importantly, in

contrast to resistivity effects which are a measure only of the number of defects present, elastic constants have the advantage of being sensitive to the symmetry of the defect strain field as well. Thus defect induced elastic constant changes should serve as a means for investigating the configurations assumed by various defects in the host lattice. In particular then, a study of these effects is especially important in view of the controversy concerning the geometrical nature of the I_E defect which still exists after years of considerable theoretical and experimental effort.

Point defects are expected to contribute to the elastic properties of metals in at least four ways: (1) a bulk effect due to the alteration in number and strength of inter-atomic bonds, (2) relaxation effects which involve a thermally activated reorientation of the defect under an applied stress, (3) polarization effects which occur if the defect is strongly polarizable by an external stress, and (4) dislocation pinning effects. A fifth mechanism directly related to the polarization effect and apparently hitherto overlooked will be discussed later in the thesis.

An early theoretical calculation by G. J. Dienes[4] indicated that the bulk effect would increase all the ordinary elastic constants of copper by about 10% per atomic per cent interstitials, but decrease them by approximately one per cent per atomic per cent of lattice vacancies. If this is true, a measurement of the bulk effect would provide an empirical method for distinguishing between these two types of defects. Such a measurement would be very useful in the interpretation of radiation damage.

Although Dienes' calculations predict a clear cut difference in behavior for vacancies and interstitials, there are other calculations which arrive at very different conclusions. These predictions vary over two to

three orders of magnitude and even differ as to the expected sign of the effect. For example, Zener[5] offers a semi-quantitative treatment which predicts a decrease in the shear elastic constants of about 10% per atomic per cent of either vacancies or interstitials, while Nabarro's[6] linear elasticity result estimates 3.8% and -2.3% per atomic per cent of interstitials and vacancies, respectively. More recently, Melngalis[7] has given an elasticity calculation which indicates that all the elastic constants should be decreased on the order of a hundred per cent per atomic per cent of interstitials.

These calculations are all concerned with the bulk effect. A dynamic contribution to the elastic moduli will also occur if a relaxation of preferential defect orientations is induced by an applied stress. Characteristic of such an anelastic effect is a peak in the internal friction measurements and a concomitant decrease in the elastic constant. Any defect that introduces a strain field possessing lower symmetry than that of the lattice can give rise to an anelastic effect. As the relative alignment of the applied stress and defect orientation is altered, the anelastic effects contribute in varying amounts, thus revealing the symmetry of the interacting defect. These phenomena have been used extensively to investigate impurity effects in various materials[8] and two studies of the elastic moduli of copper at low temperatures have reported the existence of relaxation phenomena associated with a vacancy-interstitial complex.[9,10]

The importance of large polarization effects, which lead to correspondingly large decreases in the elastic constants, has only very recently been recognized. By using a computer simulation of the copper lattice, Dederichs *et al.*[11] have shown that the ⟨100⟩-split dumbbell interstitial

is strongly polarizable by an applied shear stress due to the large negative bending spring constants which result from the highly compressed nature of the lattice in the vicinity of an interstitial defect. These bending springs also introduce low frequency resonant modes into the vibrational spectrum of the lattice. The large negative contributions from the polarizability effect will again differ in magnitude among the various elastic constants according to the symmetry of the defect.

These effects indicate that valuable information about the lattice configurations of point defects may be obtained by studying defect induced changes in the elastic moduli. Unfortunately, the indirect effect from the pinning of dislocations by these defects can be much larger than any of the direct contributions. Under an applied stress, the motion of dislocations contributes a plastic strain which decreases the effective elastic constants from their perfectly elastic values. Vacancies and interstitials distort the lattice, introducing strain fields which can interact with the dislocation array and cause pinning of the line segments; the strain ascribable to dislocation motion is thereby eliminated and the measured elastic constants are increased. An investigation of this effect in the Young's modulus of copper has found an initial million-fold increase per atomic per cent interstitials.[12] Because of this considerably larger contribution expected from dislocation pinning, it is imperative that dislocations be eliminated in any attempt to accurately determine the magnitude of the other effects.

Hence, although elastic constants measurements promise to be very useful for the determination of defect properties, the theoretical treatment of elastic defect effects is uncertain, and the large dislocation contributions make the measurement very difficult. Furthermore, even in those

experiments which have attempted to isolate the contributions due to dislocations, large differences (which span practically the same range as the theoretical estimates) exist between the various investigations. After an extended irradiation of a single crystal copper rod at 4 K with reactor neutrons, Thompson et al.[12] found no change in the Young's modulus of the rod, indicating an effect of less than a one per cent change per atomic per cent of Frenkel defects. Dieckamp and Sosin[13] reported a decrease in the shear constant of a thin polycrystalline copper foil of (-7±3)% per atomic per cent Frenkel pairs after electron irradiation near 80 K. Konig[14] et al. also irradiated a thin polycrystalline copper foil, using alpha particles at 4 K, and observed a 140% decrease in the shear constant per atomic per cent of Frenkel pairs. Furthermore, they gave a corrected value of the Dieckamp and Sosin results which agreed with their own work. Townsend[9] et al. report a change of (-13±3)% per atomic per cent of defects in the Young's modulus of Cu and W foils irradiated with 10 mev protons below 15 K, while Roth and Naundorf[15] found a decrease in the Young's modulus of copper of 75% per atomic per cent Frenkel defects after electron irradiation at 120 K. Okuda and Nakani[16] were not able to directly observe the effect in copper after fast neutron irradiation below 15 K but concluded it must be less than -80% per atomic per cent Frenkel pairs. Wenzl et al.[17] give values of -47%, -39%, -67%, for Al, Cu and Pt foils, respectively, irradiated at 8 K with reactor neutrons. However, Nielsen and Townsend[9] apparently found no such large effect after bombarding both single and polycrystalline copper foils at liquid helium temperatures with protons. They did find a very large relaxation modulus effect which they associate with the reorientation of the defect responsible for either stage I_B or I_C annealing. Ehrensperger

et al.[10] also observed this relaxation and concluded that it probably was due to the stage I_C defect.

There are several possible explanations for this wide range of experimental disagreement. One of the more apparent is the uncertainty of the defect concentration in several of the experiments. The most direct measurement of concentration is furnished by electrical resistivity, but of the above investigations only those of Roth et al.[15] and Ehrensperger et al.[17] included simultaneous resistivity measurements. Another possibility is that the different elastic constants measured by the various investigators do not have the same functional dependence on defect concentration. Only one reported investigation has been made of the change in all three independent cubic elastic constants as a function of defect production; Gerlich et al.[18] performed the measurements on LiF at room temperature. This material is expected to give results similar to copper because Born-Mayer repulsion terms contribute strongly to the elastic characteristics of both solids. However, all the elastic constants were found to decrease uniformly with the introduction of defects and no large changes were observed.

The presence of relaxation effects, which are negative and may be large, is another possible explanation. Such contributions are in general sensitive to the type of damage created in the lattice, the elastic constant being considered, and the frequency and temperature of measurement. These effects may in principle be observed by measuring the temperature or frequency dependence of either the internal friction or elastic modulus. Although anelastic effects have been reported, no systematic investigation has been made of their possible contributions. In fact, practically all of the reported studies were conducted at a fixed temperature and frequency, thus

completely negating any opportunity to separate relaxation effects from other contributions.

Finally, the effects on the elastic constants are probably sensitive to the nature of the defects which are generated. Isolated vacancies, interstitials and close-pairs should all produce different effects, so that irradiations with different particles or at different temperatures would be expected to produce different results. This question will be one of the principal concerns of the thesis.

The purpose of this thesis is therefore an investigation of the relative importance of the different contributions to the elastic constants of copper from stage I defects. The experiments consist of measurements at 10 MHz of the irradiation induced changes in all three independent elastic constants, the determination of their annealing behavior through stage I and their measurement as a function of temperature in search of anelastic effects. Simultaneous measurements of the attenuation and resistivity will be used to monitor the defect concentration.

The use of 10 MHz sound waves has many distinct advantages over the lower frequency (10 to 10,000 Hz) range utilized in the studies mentioned above. Only longitudinal constants can be measured by the resonant bar (and complicated analytical expressions determine the elastic moduli measured with the cantilevered beam) techniques employed at the lower frequencies; there is also the problem of ascertaining the effects from various clamping procedures necessary to support the cantilevered samples. In contrast, the pulse-echo method appropriate for the megacycle range enables the changes in all ordinary constants to be easily measured with high sensitivity. Because the sample itself is not forced into resonance, there is no need for it to be

clamped. Due to the fact that all sample dimensions must be large in relation to the wavelength of the experimental frequency, the pulse-echo technique is not sensitive to surface effects.

The method is also more convenient for separating low temperature relaxation phenomena from the bulk contribution. For example, at kilohertz frequencies the anelastic effect first reported by Nielsen et al.[9] appears to be a significant contribution even as low as 10 K. The peak of this relaxation should occur as the frequency of the applied stress nears the jump frequency of the defect, so the temperature dependence of the resonant frequency, V_R, is given by an Arrhenius expression[19]:

$$V_R = V_0 e^{-E_m/kT} .$$

Here E_m is the activation energy for motion of the defect and V_0 is an effective frequency which approximates the oscillation rate of the defect in its equilibrium position toward the saddle point. Using the value found by Nielsen and Townsend[9] for E_m, 0.015 eV, this expression indicates the process should shift upwards in temperature to approximately 18 K. Hence the contribution from the relaxation should be decreased significantly at the lower temperatures, and the bulk contribution can more easily be separated from the relaxation effect.

Because of the large relative size of the sample (approximately 1 cm^3) most appropriate for the pulse-echo technique, only neutron irradiation is capable of creating both a homogeneous distribution and adequate concentration of defects. However, fast neutrons create large depletion zones in the lattice which may complicate the direct study of simple point defects. Accordingly, the irradiation in the present experiments was

performed with thermal neutrons. These particles create displacements through (n,Y) capture reactions, rather than by direct knock-ons. Isochronal annealing studies of resistivity changes from this type of damage exhibit greater recovery and sharper annealing peaks than are observed for fast neutron bombardment. This is indicative of isolated close-pairs, vacancies and interstitials, and consistent with the low recoil energy (100 to 500 ev) given the emitting nucleus.[20] However, because of the lower damage rates obtainable with presently available fluxes, the use of thermal neutrons does not permit elimination of dislocation contributions by the usual method of irradiating until they become saturated. Therefore, it was necessary that this pinning be effected prior to the final irradiation.

There are several reasons for using copper in the investigation. High purity samples are easily obtained and it has been the subject of much previous study. Its cross-section for thermal neutron capture is large enough to allow both resistivity and elastic constant changes to be accurately measured in a reasonable length of time. The mean free path characteristic of thermal neutrons in copper is also large enough (about 3 cm) to give a homogeneous distribution of damage. Because the inter-atomic potential of copper is primarily determined by a simple Born-Mayer interaction,[21] most theoretical calculations have been based on this material. An additional reason is the availability of low-dislocation-density samples[22] which may be important in eliminating dislocation effects.

The experimental conditions necessary for this investigation also permitted very accurate and dislocation-free measurements of the temperature dependence for all three independent copper elastic constants over the range from 3.6 to 45 K. Recent calculations by Garber and Granato[23] have

generated interest in just such results. Their work predicts a T^4 dependence of the moduli over this range, but disagrees with the only existing measurement which is accurate enough to be compared to the theory. The results of these measurements are also presented and discussed in this thesis.

Section II of this thesis is a description of the equipment and techniques which were used in the investigation. The experimental results are presented in section III, section IV contains a discussion of the results, and a summary is given in section V.

II. EXPERIMENTAL TECHNIQUES AND APPARATUS

The three single crystals of 99.999% copper were prepared by Dr. F. W. Young, Jr., at the Oak Ridge National Laboratory. The details of this procedure have been described previously.[22] Three cubes approximately 12 mm on a side, with faces perpendicular to the [100], [011] and [01$\bar{1}$] directions, were each cut by an acid saw technique[24] from a 1" diameter cylinder about 15 mm long, and then annealed at 1050°C for 10 days to minimize the number of dislocations. The normal dislocation density of crystals prepared by this technique is extremely small, on the order of $10^3/cm^2$ or less. The samples were subsequently radiated at room temperature to an integrated dose of 10^{17} nvt fast neutrons to pin the few remaining dislocations and harden the crystals.

Flat and parallel surfaces are required for ultrasonic measurements in order to avoid interference effects. Since the usual method for doing this (hand lapping the samples using abrasive powder on a granite block) introduces new, unpinned, dislocation segments, a chemical polishing technique was used. The method is designed to create optically flat and parallel surfaces without the introduction of any dislocations.

A polishing holder like the one shown in Fig. 1 was used. The two pieces of this holder were carefully machined so that the bottom surface of the upper plug sat parallel to the plane on which the Delrin legs rested. These legs were mounted on the piece prior to final machining to insure proper alignment. The two pieces were made to fit snugly, but allowed to slip freely in the vertical direction. The adjacent surfaces were lubricated with Dow Corning Spray-Kote Bonded Lubricant. The sample

Fig. 1. Sample holder used for chemical polishing of the samples. Diameter is approximately $3\frac{1}{2}$ inches.

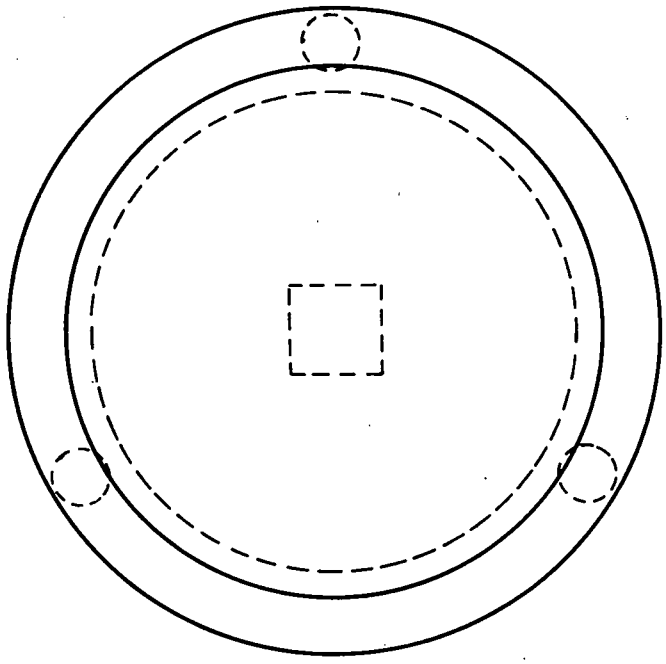

Top View

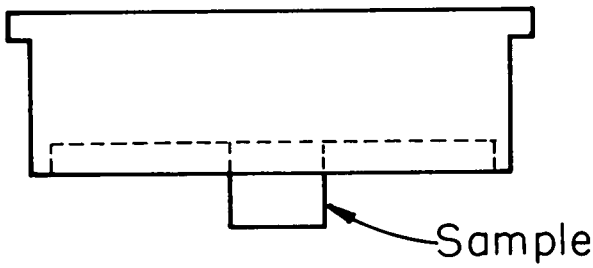

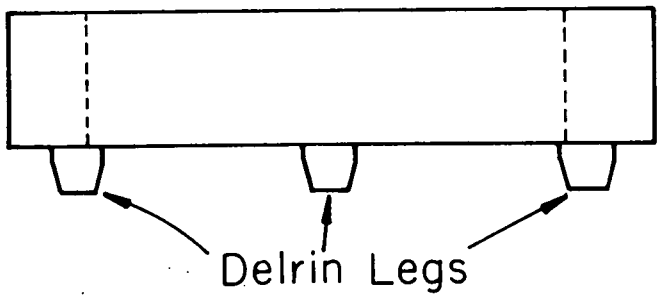

Side View

Fig. 1. Sample holder used for chemical polishing of the samples. Diameter is approximately $3\frac{1}{2}$ inches.

was then mounted on the bottom surface of the plug, using a very thin layer of phenyl salicytate (salol).

Flat laps necessary for the polishing were prepared by tightly stretching thin percale sheeting (approximately 200 threads/inch) over rectangular glass plates (about 1' X 2' X 3/16"). It was essential to keep all materials scrupulously clean to avoid scratching the sample. Two solutions, based on the work of J. W. Mitchell and co-workers[25,26] at the University of Virginia, were mixed. Solution A consisted of 90 ml of concentrated hydrochloric acid and 10 ml of polyethylene glycol 400 saturated with cupric chloride. Solution B was made from 200 ml each of concentrated hydrochloric, glacial acetic and orthophosphoric acid, and 60 ml of polyethylene glycol 400. The solutions were kept in tightly sealed bottles and all polishing work was done under a fume hood.

A lap was readied by saturating the left half with solution A and the right with solution B. A microscope slide was used to mix the solutions on the lap so that a gradual transition from left to right of pure A to pure B was achieved. All excess liquid was scraped away. The sample holder containing the mounted specimen was placed down on the left half of the lap. The holder was then gently slid up and down on the lap and gradually moved from left to right and finally back to the left. By gripping just the outer portion of the holder, the only significant stress on the crystal was created by the relatively small mass (approximately 200 gms.) of the aluminum plug. The sample always remained in direct contact with the cloth. The entire holder was then carefully lifted from the lap, and the crystal was immediately flushed with alcohol and dried in a stream of N_2 gas. The entire procedure took just a few minutes and was repeated, usually only once or twice, until

the face appeared flat and free from scratches. The crystal was then removed from the holder by gently heating it to about 60°C, cleaned with alcohol and acetone, and remounted so that the opposite face could be polished. After this, the orientations of the faces were checked by taking back reflection Laue photographs and using the double exposure method of Ochs.[27] All faces were found to be within 1° of the desired direction. In this manner, a set of flat and parallel (100) faces was prepared on crystals 1 and 2, and a set of (110) faces for crystal 3.

The measurements were taken in the Low Temperature Irradiation Facility at Oak Ridge National Laboratory; detailed descriptions may be found elsewhere.[28] It provides a relatively pure thermal neutron spectrum of high flux at the liquid helium temperatures necessary to immobilize point defects. This facility has been used extensively to investigate resistivity changes in many different materials.[29] The one by eight inch cylindrical sample chamber lies at the bottom of an 18 foot long tube. Three identical rigs for holding the samples were constructed as shown in Fig. 2. These rigs allowed refrigeration of the sample and contained all the necessary electrical leads. The flexible bellows permitted the rig to be bent for more easy transportation.

Fig. 3 shows how the crystal and resistivity samples were mounted in the chamber at the bottom of the rig. A 3/8", 10 megahertz quartz transducer, X-cut for sample 1 and AC-cut for samples 2 and 3, was bonded to one polished face of each crystal. Nonaq, a commercially available stopcock grease appropriate for low temperatures, was used as the bonding agent. A spring loaded aluminum plunger held the transducer and sample firmly in place and also provided an electrical contact to the transducer. Aluminum was utilized

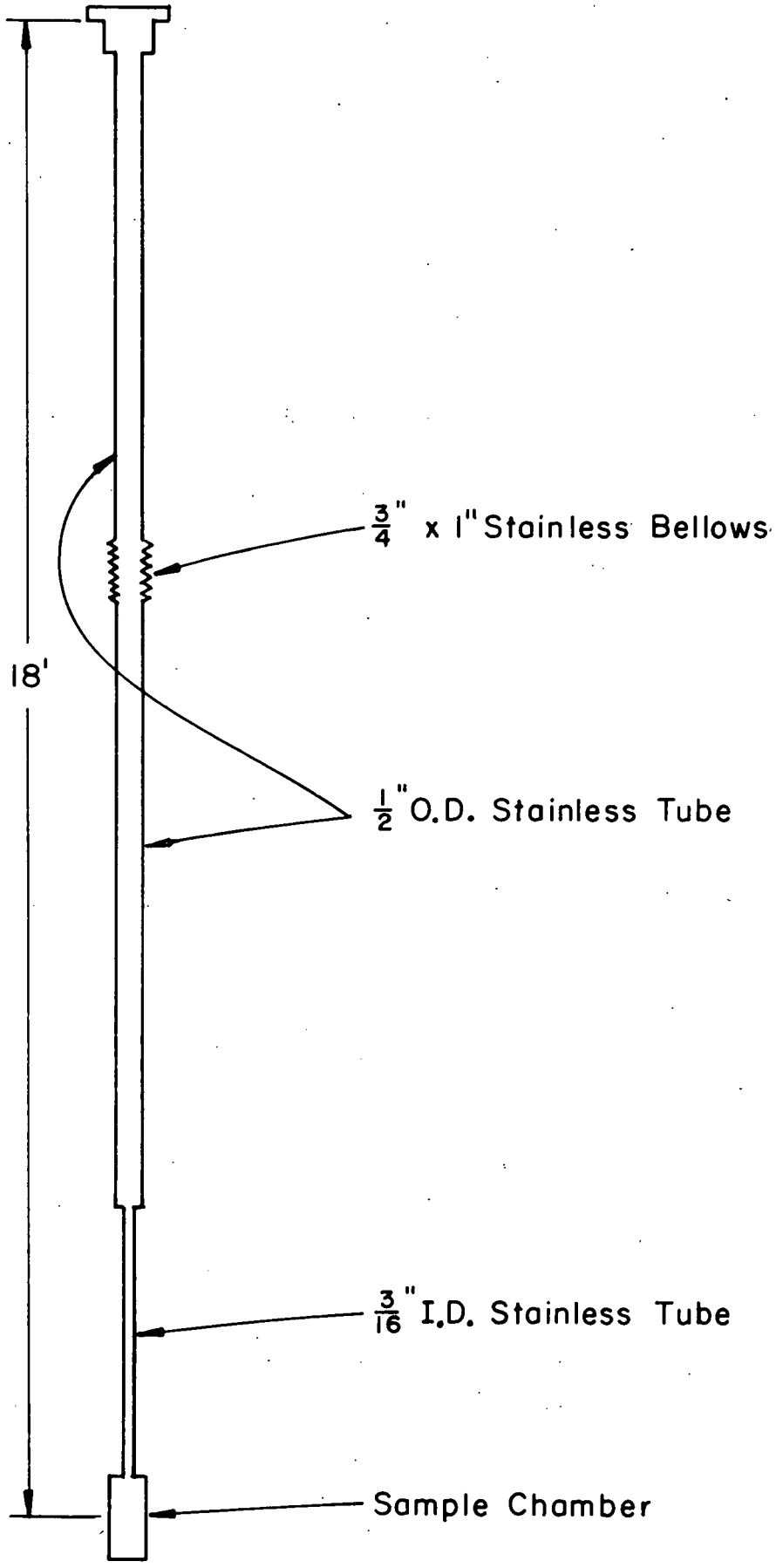
18'
3/4" x 1" Stainless Bellows
1/2" O.D. Stainless Tube
3/16" I.D. Stainless Tube
Sample Chamber

Fig. 3. Sample chamber. The location of various components has been indicated by appropriate arrows. The height of the chamber is approximately 4 inches.

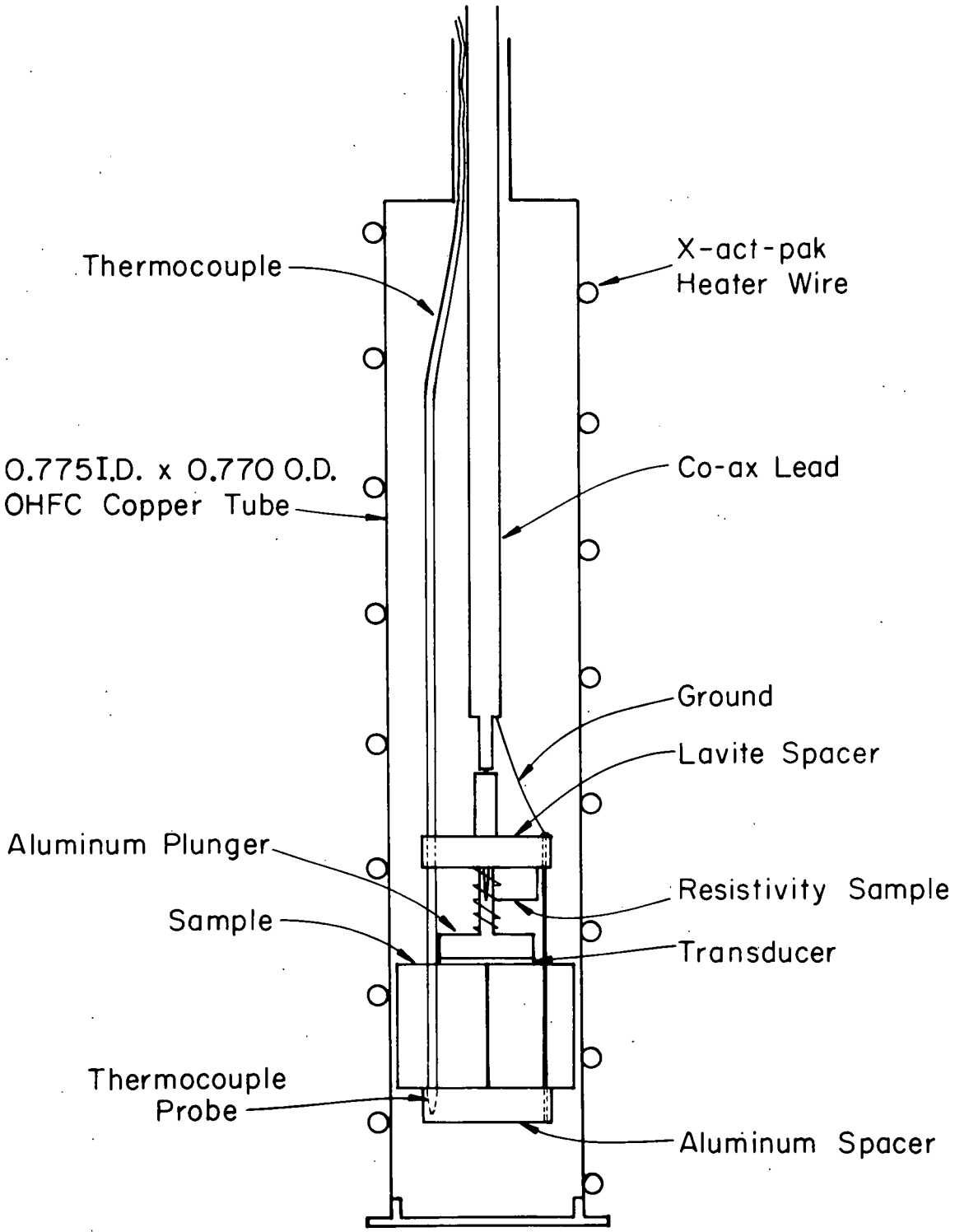
Thermocouple
X-act-pak
Heater Wire
0.775I.D. x 0.770 O.D.
OHFC Copper Tube
Co-ax Lead
Ground
Lavite Spacer
Aluminum Plunger
Resistivity Sample
Sample
Transducer
Thermocouple
Probe
Aluminum Spacer

wherever possible in the chamber because of its low cross section for thermal neutron capture.

Two types of thermometry were used in the experiment. Irradiation and reference temperatures, always below 4 K, were determined by measuring the vapor pressure of the liquid helium in which the sample was immersed. A copper-constantin thermocouple was used to measure the elevated temperatures. The tip of the thermocouple was coated with a thin layer of GE No. 7031 Insulating Varnish and epoxied with Stycast to the aluminum plate in direct physical contact with the sample. This epoxy has a relatively high thermal conductivity; the varnish was used to electrically insulate the thermocouple from the metal crystal.

Small rectangular pieces, approximately 0.5" long and 0.002 in^2 in cross-section, were acid cut from parts of the original single crystals to be used as resistivity samples. Three of these were etched down with nitric acid to reduce this relatively large a/l ratio. One of these was mounted in each holder and connected with current and potential leads as shown in the figure. A 30" length of x-act-pac heater wire was carefully soldered to the outside of the sample can and electrically connected to a Kovar feed-through at the top of the rig. This heater was used to supply energy for the annealing pulses.

The velocity and attenuation system used was that discussed previously by Holder[30] and Read and Holder.[31] The velocity measurement is based on the McSkimin pulse superposition technique[32]: pulses gated from a continuous wave are applied to the sample at time intervals of approximately twice the round trip transit time of the signal, resulting in a superposition of all the odd echoes. This superposition is maximized when the round trip

transit time is a half integer multiple of the period of the continuous wave, corresponding to constructive interference. Small velocity changes can be determined by the frequency change necessary to reachieve the maximum superposition. Attenuation values are obtained by periodically interrupting this interference condition and measuring the ratio of two successive pulse amplitudes. On a specimen of normal attenuation, this system has simultaneously detected velocity changes of one part in 10^7 and attenuation changes of 0.001 db/usec. Runs made during the experiment without irradiation showed the velocity as measured by the system to be stable within plus or minus 2 parts in 10^7 over a period of two days.

After the rigs were lowered into position, a room temperature resistivity reading was taken and the sample chamber was cooled to liquid helium temperatures. This took approximately two hours. The slow cooling was used to lessen the risk of introducing new dislocations because of the differing thermal expansion coefficients of the quartz and copper. This risk was further minimized because the bonding agent, Nonaq, does not solidify until well below room temperature. Readings were then made of the resonant frequency and attenuation at various temperatures between 3.6 and 45 K. These readings determine the "normal" temperature dependence of the attenuation and elastic constant. The sample can was then filled with liquid helium, and frequency, attenuation and resistivity were recorded at the reference temperature (approximately 3.6 K). The reactor was subsequently turned on and taken to full power in a period of a few minutes. The resultant heating caused the irradiation temperature to be a few tenths of a degree above the reference temperature. The attenuation and resonant frequency were monitored continuously and resistivity measurements were made periodically

during the bombardment. The length of time necessary for each run was determined by the rate of damage production in the sample. An average run was about 50 hours. This was considerably longer than needed to measure the effect during irradiation, because a much higher degree of sensitivity was needed to accurately determine the annealing behavior.

The annealing program consisted of pulsing the sample to an elevated temperature (usually for a period of 15 minutes), taking measurements of attenuation and resonant frequency at the pulse temperature, then cooling to the reference point and again recording the attenuation and frequency, and here also the resistivity. The long pulse duration was to ensure the attainment of thermal equilibrium, which is necessary for an accurate frequency reading. These initial "at temperature" values include both temperature dependent and annealing effects. In order to simplify the interpretation of possible temperature dependent effects which might be introduced by the irradiation, a number of "at temperature" measurements were also made for temperatures below that of the annealing pulse after the pulse was completed; such readings should be free of annealing effects.

III. RESULTS

A. Effects Observed at Liquid Helium Temperatures

The changes in resonant frequency measured during each of the five different thermal neutron bombardments are plotted as a function of irradiation time in Figs. 4-8; the total resistivity change introduced by each irradiation has been printed on the appropriate figure. During every run, resistivity changes were observed to be linear in irradiation time.

Figs. 4 and 5 show the results obtained from two different runs involving the C_{44} mode. This crystal was annealed to 320 K prior to the second run. The marked linearity and reproducibility evident in these results demonstrate the high degree of accuracy and sensitivity attainable with the pulse superposition method and give good evidence that dislocation effects were not a contributing factor.

Because of the quality of the data obtained for sample two, only one irradiation was performed with the C' mode. These results are presented in Fig. 6. Again the linearity of the measurements is striking.

Experiments involving the longitudinal mode for measuring C_{11} (Figs. 7 and 8) were the most difficult to perform. Not only was the effect small, but sporadic jumping of the frequency began sometime after the first irradiation. These unexplained jumps varied in magnitude from 10 to 50 cycles and were always positive. Figure 7 is for the entirety of the first irradiation, where no jumping was observed. The next figure, Fig. 8, is for nine hours near the end of the almost 138 hours of the second run. This period was the longest monitored portion of the run which exhibited no jumps. The excellent agreement between these two results, along with evidence from other shorter periods during the irradiation where no jumping occurred, indicates that this measurement of the effect is a reliable one.

Fig. 4. The measured change in resonant frequency observed during irradiation below 4 K, plotted versus the irradiation time for the first C_{44} run. The total irradiation produced change in the electrical resistivity during this run was measured to be 1.230×10^{-3} μ-Ω-cm.

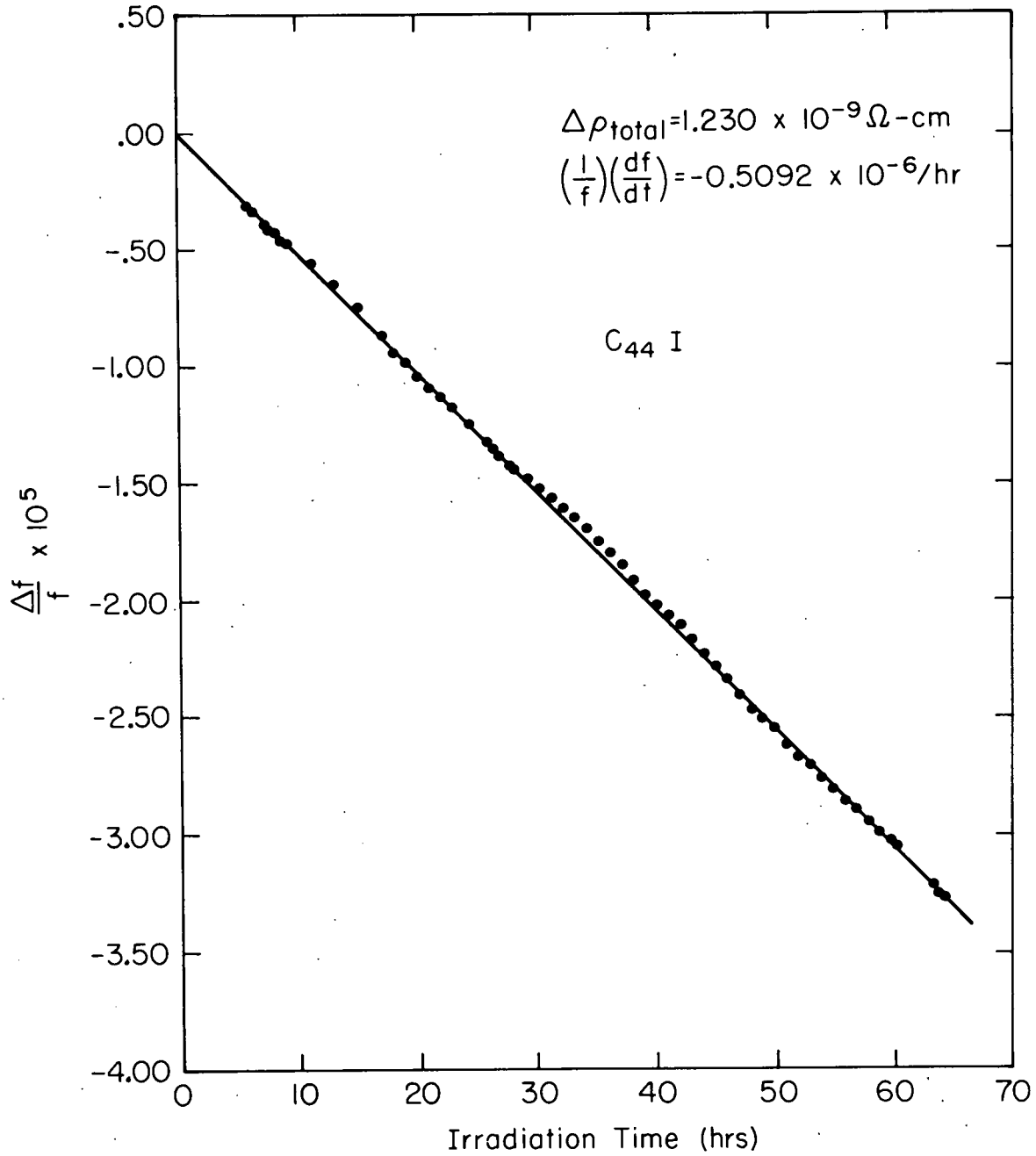
.50
.00
-.50
-1.00
-1.50
-2.00
-2.50
-3.00
-3.50
-4.00
0
10
20
30
40
50
60
70
Irradiation Time (hrs)
$\frac{\Delta f}{f} \times 10^5$
$\Delta\rho_{total}$=1.230 x 10^{-9} Ω-cm
$\left(\frac{1}{f}\right)\left(\frac{df}{dt}\right)$=-0.5092 x 10^{-6}/hr
C_{44} I

Fig. 5. The measured change in resonant frequency observed during irradiation below 4 K, plotted versus the irradiation time for the second C_{44} run. The total irradiation produced change in the electrical resistivity during this run was measured to be 0.916×10^{-3} μ-Ω-cm. This sample was annealed to 320 K prior to the second run.

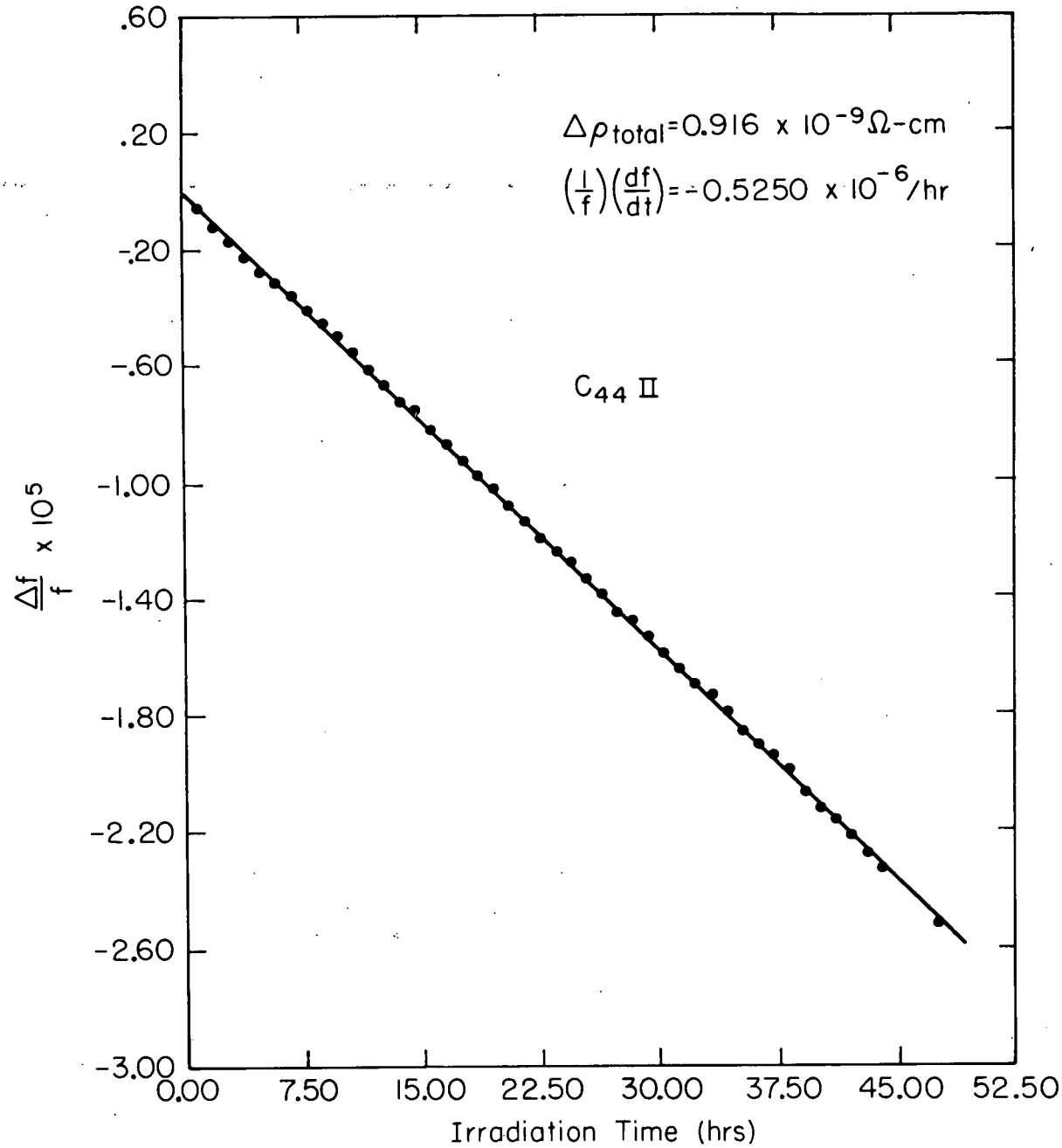
.60
.20
-.20
-.60
-1.00
-1.40
-1.80
-2.20
-2.60
-3.00
0.00
7.50
15.00
22.50
30.00
37.50
45.00
52.50
Irradiation Time (hrs)
Δf/f x 10^5
Δρ total=0.916 x 10^-9 Ω-cm
(1/f)(df/dt)=-0.5250 x 10^-6/hr
C44 II

Fig. 6. The measured change in resonant frequency observed during irradiation below 4 K, plotted versus the irradiation time for the C' run. The total irradiation produced change in the electrical resistivity during this run was measured to be 0.807×10^{-3} μ-Ω-cm.

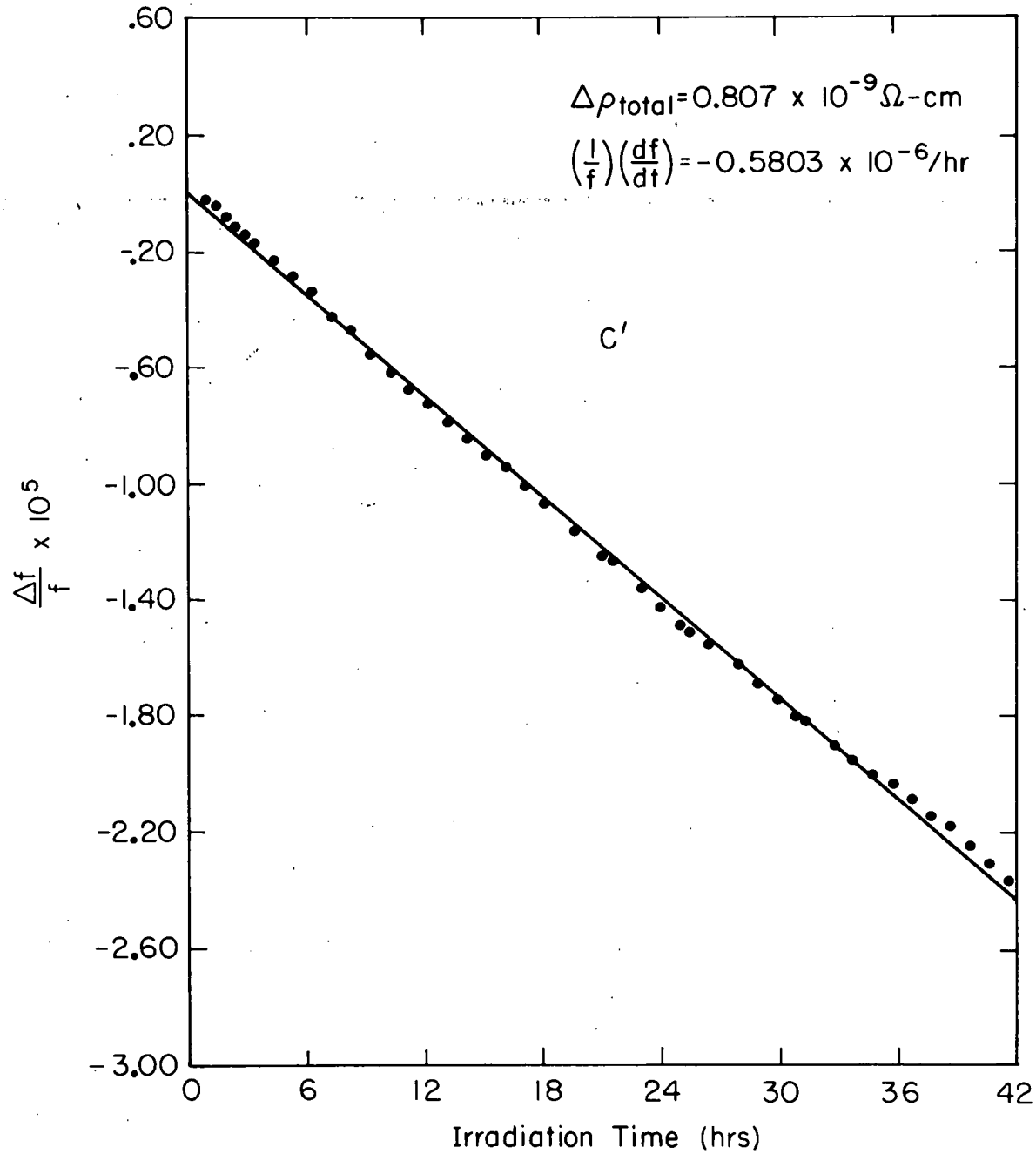
.60
.20
-.20
-.60
-1.00
-1.40
-1.80
-2.20
-2.60
-3.00
0
6
12
18
24
30
36
42
$\frac{\Delta f}{f} \times 10^5$
Irradiation Time (hrs)
$\Delta\rho_{total} = 0.807 \times 10^{-9}\ \Omega\text{-cm}$
$\left(\frac{1}{f}\right)\left(\frac{df}{dt}\right) = -0.5803 \times 10^{-6}/hr$
C'

Fig. 7. The measured change in resonant frequency observed during irradiation below 4 K, plotted versus the irradiation time for the first C_{11} run. The total irradiation produced change in the electrical resistivity during this run was measured to be 0.435×10^{-3} μ-Ω-cm.

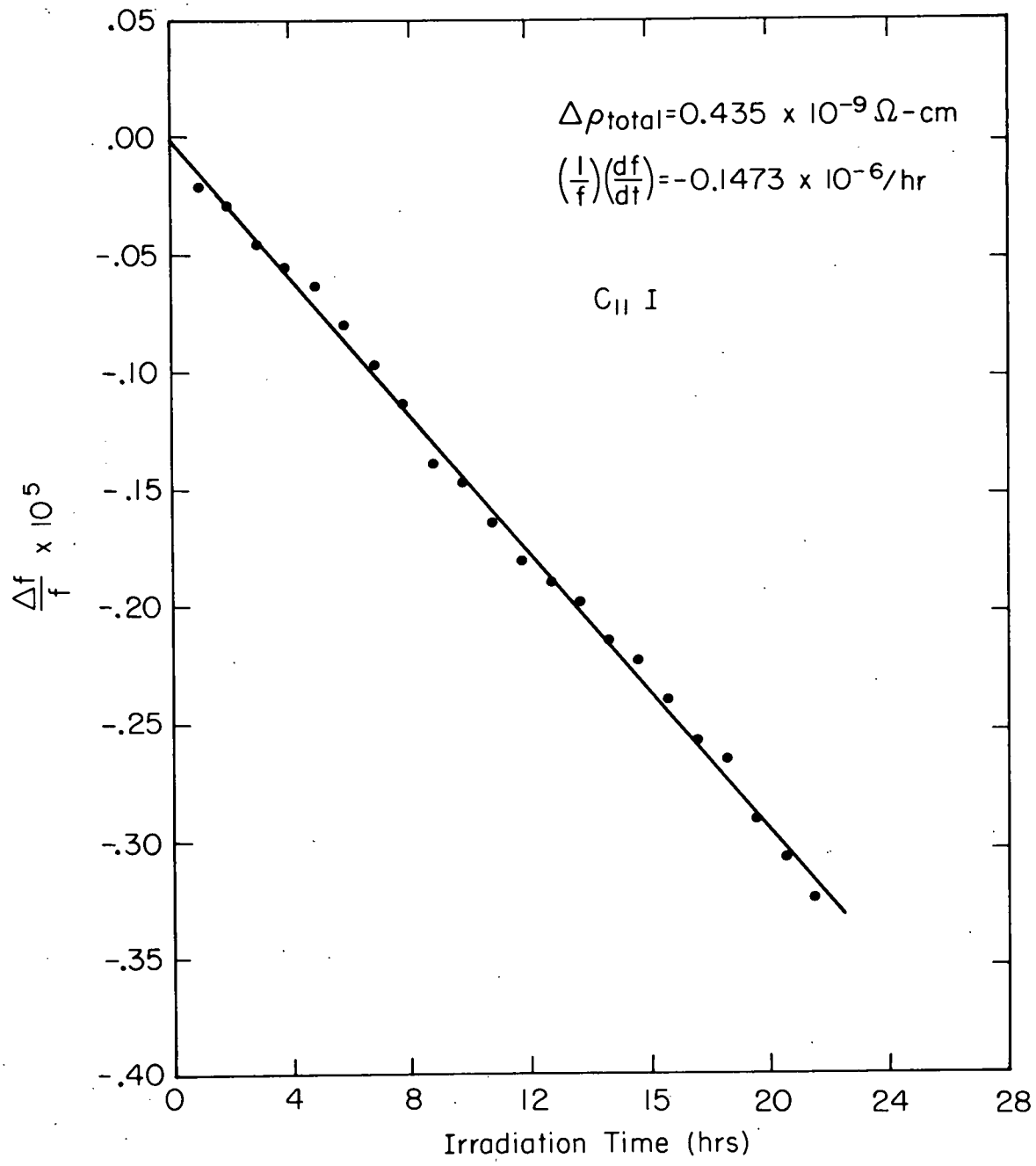
.05
.00
-.05
-.10
-.15
-.20
-.25
-.30
-.35
-.40
0
4
8
12
15
20
24
28
Irradiation Time (hrs)
$\frac{\Delta f}{f} \times 10^5$
$\Delta\rho_{total}=0.435 \times 10^{-9}\ \Omega\text{-cm}$
$\left(\frac{1}{f}\right)\left(\frac{df}{dt}\right)=-0.1473 \times 10^{-6}/hr$
C_{11} I

Fig. 8. The measured change in resonant frequency observed during irradiation below 4 K, plotted versus the irradiation time for nine hours of the second C_{11} run. The total irradiation produced change in the electrical resistivity during this run was measured to be 2.654×10^{-3} μ-Ω-cm.

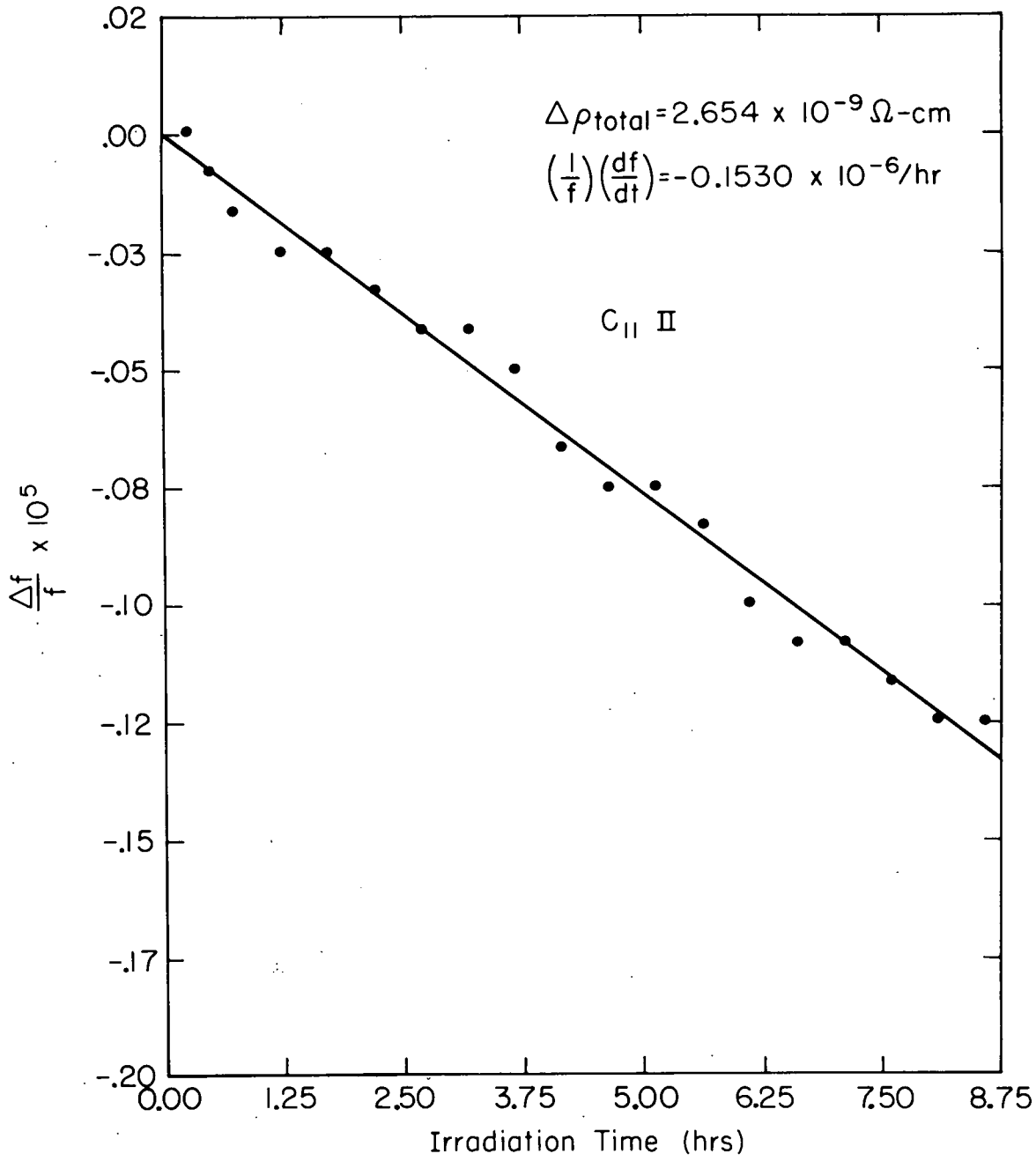
.02
.00
-.03
-.05
-.08
-.10
-.12
-.15
-.17
-.20
$\Delta\rho_{total} = 2.654 \times 10^{-9}\ \Omega$-cm
$\left(\frac{1}{f}\right)\left(\frac{df}{dt}\right) = -0.1530 \times 10^{-6}$/hr
C_{11} II
$\frac{\Delta f}{f} \times 10^5$
0.00
1.25
2.50
3.75
5.00
6.25
7.50
8.75
Irradiation Time (hrs)

As discussed in section II, the pulse superposition system used in these experiments measures a resonant frequency. A change in this frequency, Δf, corresponds directly to a change in the transit time, Δt, of the sound wave in the sample

$$-\frac{\Delta f}{f} = \frac{\Delta t}{t} = \frac{\Delta \ell}{\ell} - \frac{\Delta v}{v} \quad . \tag{2}$$

Here ℓ is the length of the sample and v represents the sound velocity. This velocity is related to the appropriate elastic constant, C, by

$$C = \rho_d v^2 \tag{3}$$

where ρ_d is the density of the crystal. Therefore

$$\frac{\Delta C}{C} = -\frac{\Delta \ell}{\ell} + \frac{2\Delta f}{f} \quad . \tag{4}$$

The slopes of the curves shown in Figs. 4-8 may be converted into changes in the elastic constants by the prescription given in Eq. (4). In order to do this, it is necessary to know the change in lattice parameter which results from the irradiation. Although no direct measurement is available for the lattice expansion created by thermal neutrons, we use the value obtained by various authors[33,34,35] using deuteron irradiation. This value, in terms of the incremental change in resistivity, $\Delta\rho$, produced by the irradiation is:

$$\frac{\Delta \ell}{\ell \Delta \rho} = 1.5 \times 10^{-3} \frac{1}{\mu\Omega\text{-cm}} \quad .$$

This contribution to the resonant frequency change is small compared to the total measured effects and gives only a minor correction to the elastic constant changes.

The resulting rates of change of the elastic constants per unit concentration, γ, of Frenkel defects, $\frac{d\ell nC}{d\gamma}$, are summarized in Table 1. A value of 2.5 $\mu\Omega$-cm per atomic per cent of Frenkel defects was used to calculate the defect concentration.

Table 1

Irradiation induced changes in the elastic constants per unit concentration of Frenkel pairs.

Run	$\frac{d\ell nC}{d\gamma}$
$C_{11}I$	- 4.6
$C_{11}II$	- 4.9
$C_{44}I$	-15.5
$C_{44}II$	-16.1
C'	-18.1

These values were computed using only 89% of the total resistivity change observed during irradiation. This is based on a recent article by Coltman et al.;[36] who discuss in detail the nature of thermal neutron damage and conclude that only this portion of the resistivity change is due to the introduction of vacancies and interstitials. The remainder is due to Zn and Ni atoms which are the result of transmutations induced by certain of the capture reactions. These impurity atoms would be expected to have only a small effect on the elastic characteristics of copper since they lie adjacent to it in the periodic table. This contention is further supported by the observations of Koster et al.,[37] where the introduction of Zn produced less than a one-half of one per cent decrease in the elastic constants of Cu per atomic per cent concentration. An additional check was made by monitoring

the resonant frequency for a period of almost 30 hours immediately following the irradiation of sample III. Because the conversion of Cu^{64} to Zn^{64} or Ni^{64} occurs with a half life of 12.8 hours, any significant contribution to the elastic constant from these elements should be evident here. The frequency remained constant within ± 2 cycles over the entire period, indicating that no measurable contribution from this mechanism was present.

Simultaneous attenuation measurements were also made during irradiation in conjunction with the resonant frequency. In two of the modes, C_{11} and C', the attenuation exhibited a linear decrease as a function of irradiation time. These results are shown in Figs. 9 and 10. The initial attenuation of the C_{44} mode was considerably higher, and no systematic change was evident.

After each irradiation, the samples were subjected to an isochronal annealing program. Pulse durations were 5 minutes for the first run, $C_{11}I$, and 15 minutes for all subsequent runs. The results are given as the irradiation induced relative frequency changes $(\frac{\Delta f}{f})$ remaining at the reference temperature of 3.6 K after the appropriate annealing pulse.

The degree of reproducibility of the results is evident from a comparison of the two different C_{44} runs. This is shown in Fig. 11, where the results from the two runs have been normalized to the same defect concentration ($\Delta\rho = 1 \times 10^{-9} \Omega$-cm) in order to allow a quantitative comparison. The agreement is excellent, particularly below 35 K, and even the details of the annealing behavior are reproducible.

This provides a crucial test of whether dislocations have contributed to the results. Since dislocation effects are not linear in defect concentration, the results from the second run would differ from those of the first if

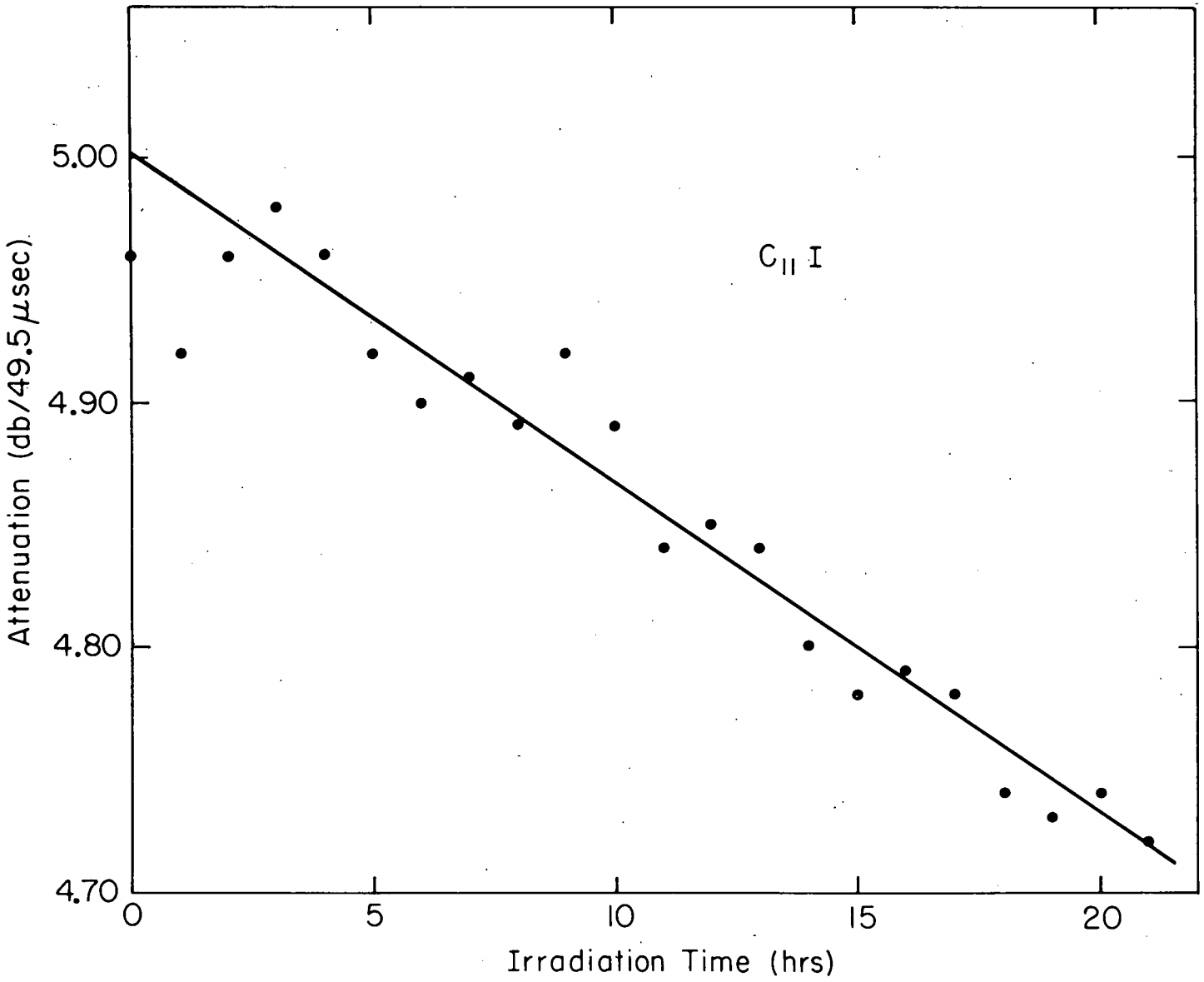
5.00
4.90
4.80
4.70
Attenuation (db/49.5 μsec)
C II I
0
5
10
15
20
Irradiation Time (hrs)

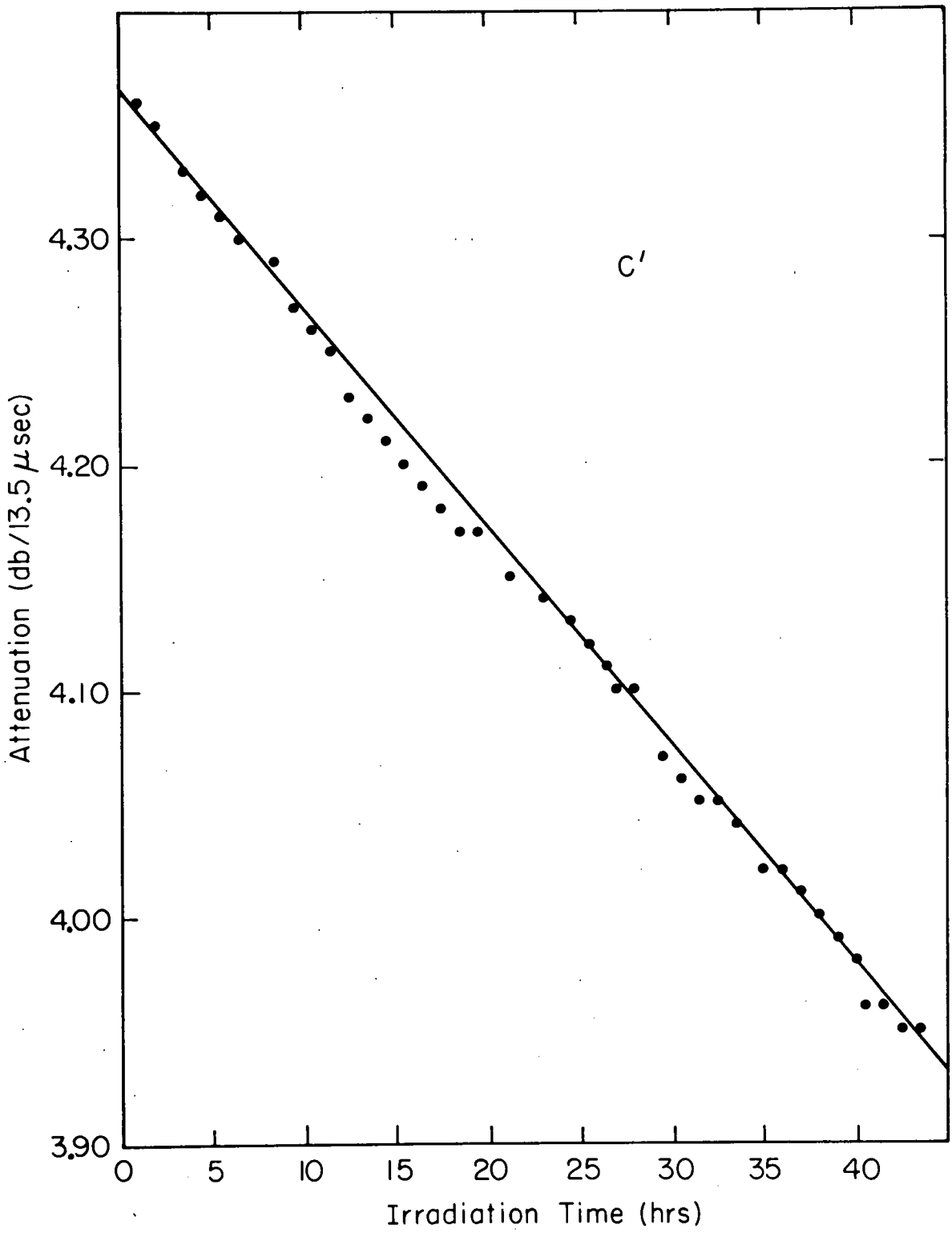
C′
4.30
4.20
4.10
4.00
3.90
Attenuation (db/13.5 μsec)
0
5
10
15
20
25
30
35
40
Irradiation Time (hrs)

Fig. 11. A comparison of the annealing behavior found during the two C_{44} runs. The results are shown as the irradiation induced relative frequency change which remains at the reference temperature of 3.6 K after various annealing pulses. The results from both runs have been normalized to the same defect concentration ($\Delta\rho=1\times10^{-3}$ μ-Ω-cm).

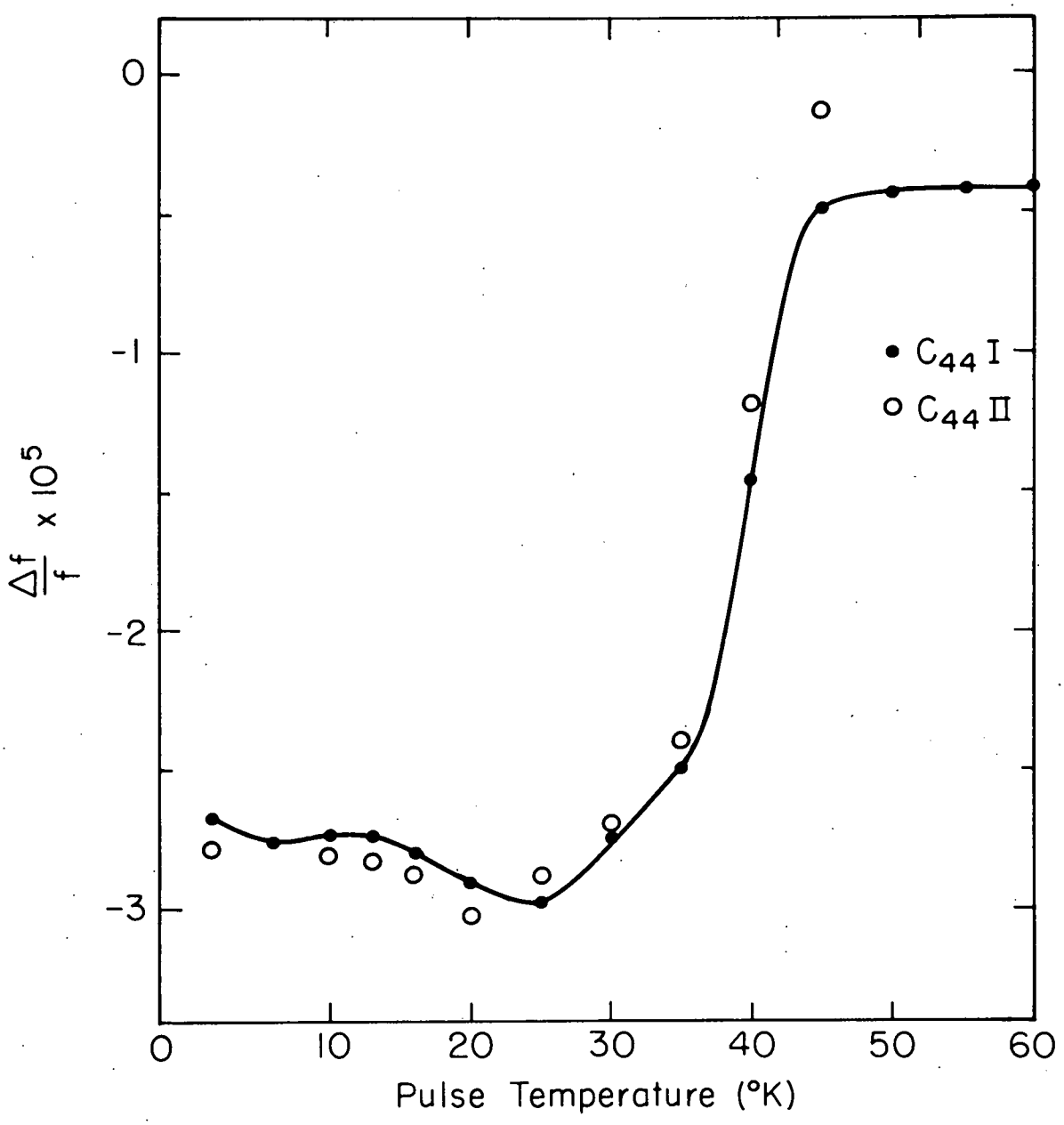
0
-1
-2
-3
$\frac{\Delta f}{f} \times 10^5$
0
10
20
30
40
50
60
Pulse Temperature (°K)
• C_{44} I
o C_{44} II

dislocations were a significant factor. More importantly, if dislocations are present in sufficient numbers to affect the low temperature (below 35 K) results, the pinning produced by defects mobile above 35 K would produce effects of a magnitude several times larger than those introduced by the bombardment. In these and all other runs the increases which resulted from the annealing of the defects were less than the decreases produced by irradiation.

The annealing of the irradiation produced relative frequency changes for all three modes is shown in Fig. 12. Two important features are evident from the plot: 1) the annealing behavior is very different for the different modes; 2) two of the constants, C_{11} and C_{44}, experience a still further decrease upon annealing. The decrease is unexpected, but apparently reproducible, as evidenced by the two C_{44} runs, and has been observed previously.[38]

The annealing of the irradiation produced attenuation changes was found to agree within experimental error (about 5%) with the resistivity recovery. This agreement is to be expected if dislocation effects have been eliminated, and will be discussed further in section IV. Fig. 13 depicts the annealing of both the resistivity and attenuation for the C' mode. The resistivity measurements obtained during the various anneals are also consistent within experimental error (approximately 1%), and closely follow the results reported for more detailed resistivity studies of slow neutron damage.[29]

B. Effects Observed above Liquid Helium Temperatures

The final phase of the measurements concerned the effects of the defects on the temperature dependence of the elastic constants. Elastic

Fig. 12. The annealing of the irradiation produced relative frequency changes measured at 3.6 K for all three elastic constants. The results from the three runs have been normalized to the same defect concentration ($\Delta\rho=1\times10^{-3}$ μ-Ω-cm).

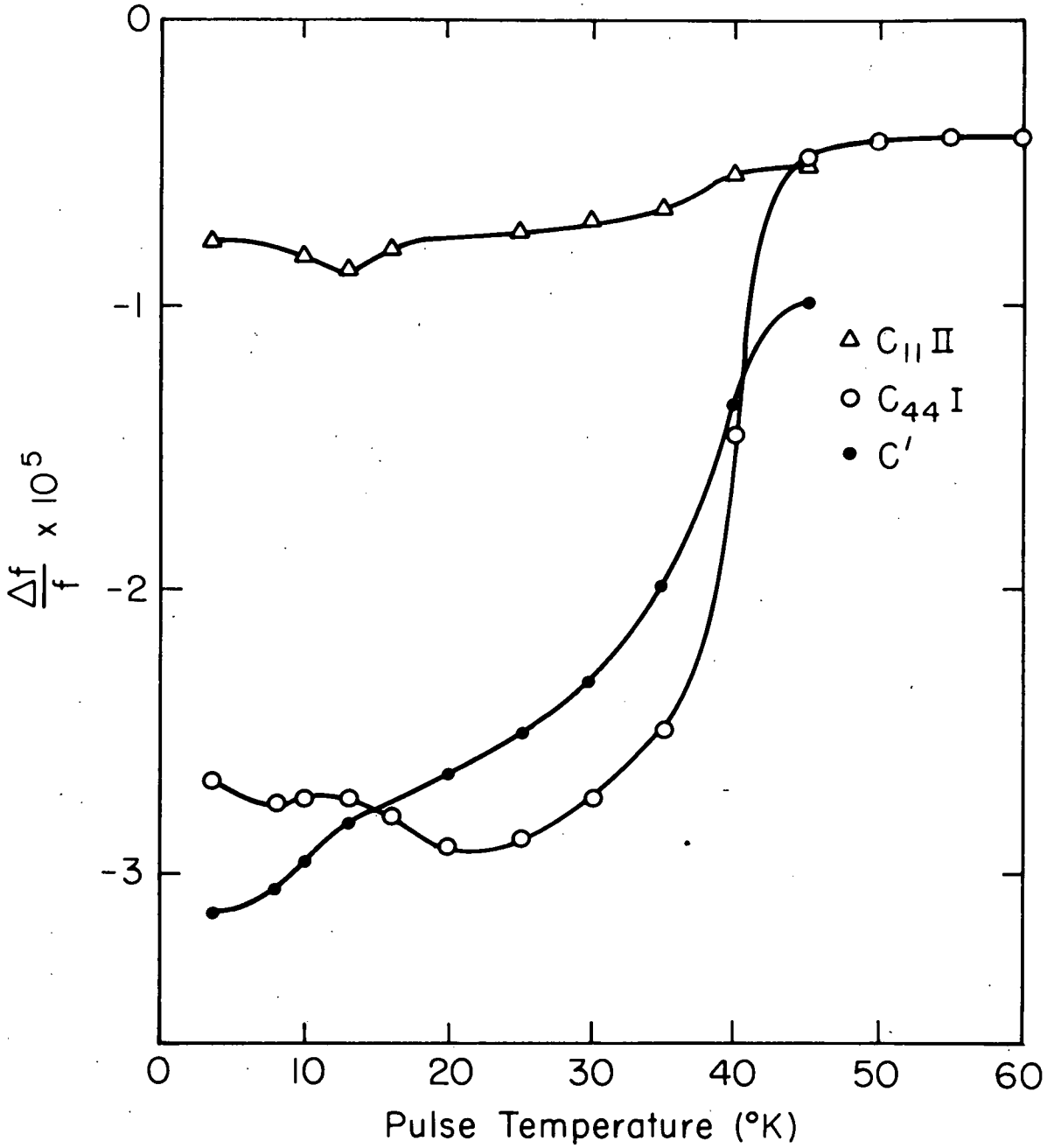
0
-1
-2
-3
$\frac{\Delta f}{f} \times 10^5$
0
10
20
30
40
50
60
Pulse Temperature (°K)
△ C_{11} II
○ C_{44} I
● C′

Fig. 13. The annealing of the resistivity and attenuation changes produced during irradiation below 4 K in the C' mode.

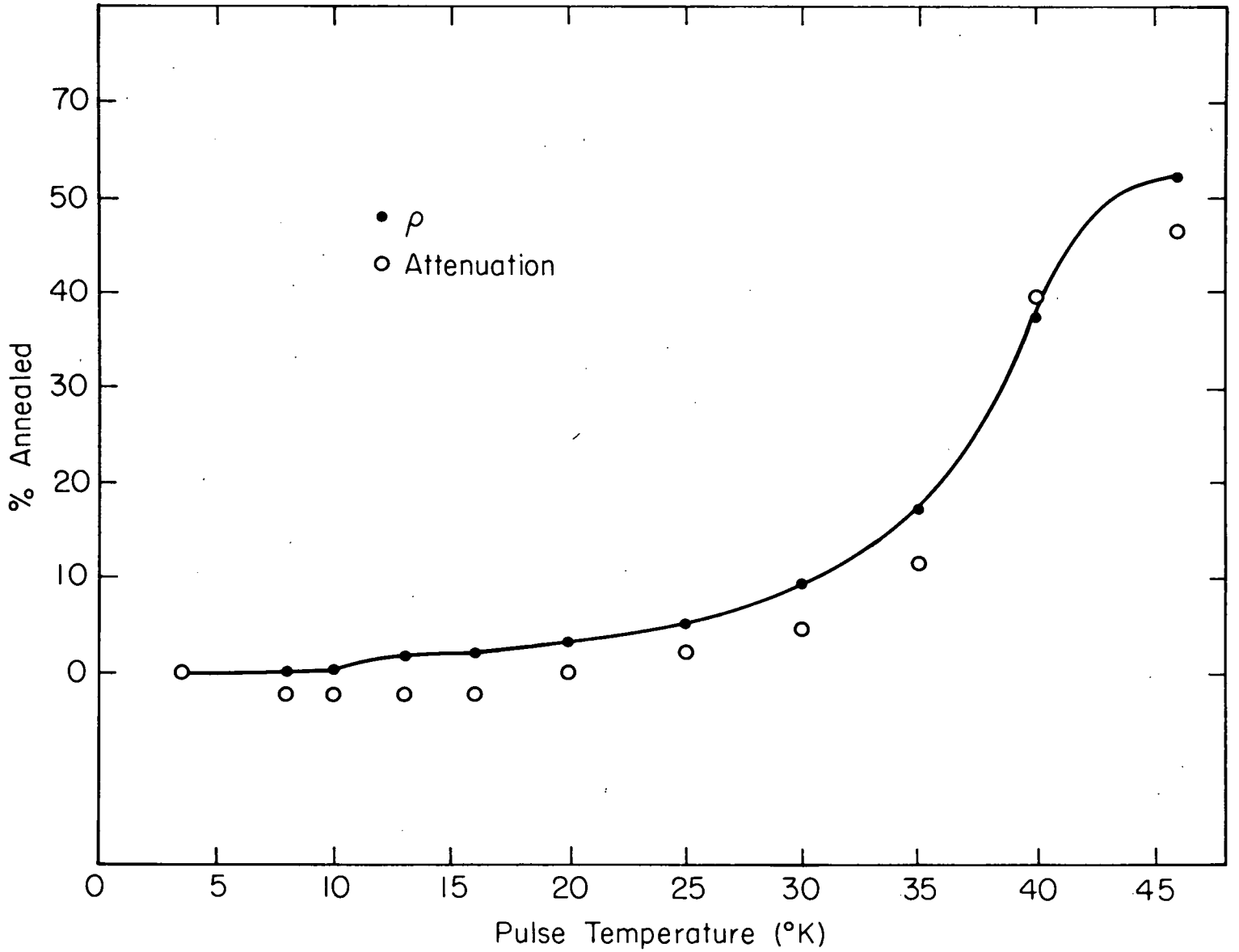
70
50
40
30
20
10
0
% Annealed
• ρ
o Attenuation
0
5
10
15
20
25
30
35
40
45
Pulse Temperature (°K)

constants are a very sensitive function of temperature, particularly above approximately 20 K. Since these changes are larger than the temperature effects expected from irradiation, it was necessary to determine the temperature dependence of the elastic constants very accurately prior to the thermal neutron irradiation. Consequently the frequency changes were measured up to 40 K for all three unirradiated samples; the results are shown in Fig. 14. The accuracy of the temperatures above 4 K, as determined by the thermocouple, should be ± 0.1 K at the lower temperatures and even better at the higher ones. Normally, the frequency at 40 K was found to be reproducible within ± 10 cycles; at 10 K, this was ± 2 cycles. Below 4 K, where the temperature was determined very precisely by the vapor pressure of the liquid helium, it was ± 1 cycle.

The results are plotted versus T^4 to facilitate comparison of the results with the predictions from a recent elasticity calculation of the temperature dependence of perfect crystal elastic constants by Garber and Granato.[23] The high precision of these results for all three constants over this temperature range provides a sensitive check of their anisotropic continuum theory, since the assumptions they made should be most valid in the low temperature regime. The straight lines indicative of the T^4 functional dependence of the constants which is predicted by the theory, fit the experimental points quite well. This agreement is in marked contrast to measurements of the C_{44} constant by Alers *et al.*,[38] in which the presence of dislocations may have been a contributing factor. In fact, the reasonable agreement of the results presented here constitutes one piece of evidence for the absence of dislocation effects.

Fig. 14. The resonant frequency changes measured at various temperatures prior to thermal neutron bombardment for all three elastic constants.

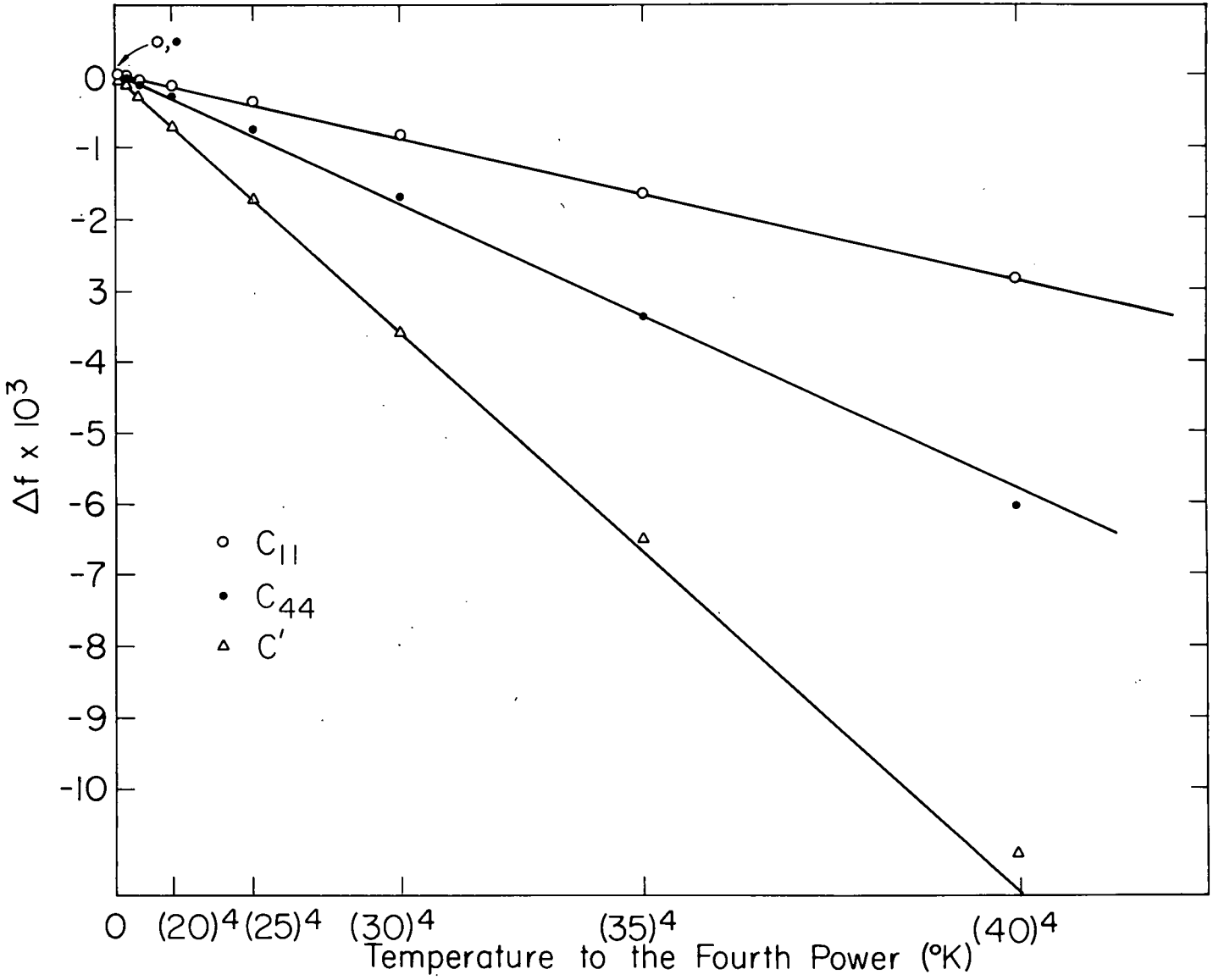
0
-1
-2
3
-4
-5
-6
-7
-8
-9
-10
Δf x 10^3
C11
C44
C'
0
(20)^4
(25)^4
(30)^4
(35)^4
(40)^4
Temperature to the Fourth Power (°K)

The difference in resonant frequency between the measurements obtained before and after thermal neutron irradiation during various stages of the 15-minute pulse annealing program for all three modes are shown in Figs. 15-18.

The first of these plots gives the results for anneals of C_{11} after the two irradiations. These curves represent points taken at each of the pulse temperatures near the end of the annealing pulse. The two runs exhibit qualitative agreement, but the two magnitudes of the effect do not scale as the total damage introduced during each run. At least four different factors could contribute to this difference in absolute magnitudes: (1) The small amount of total damage (about 40 cycles) present in the first run made accurate detection of absolute changes extremely difficult. (2) Annealing pulses for the first run were only five minutes in duration. Although this does not appear to have had a significant effect on the resistivity recovery, greater instability was evident in the frequency readings, probably as the result of a failure to achieve thermal equilibrium. (3) It is possible that one or more of the aforementioned jumps might have occurred during the annealing, and (4) the large fraction of damage from the first run still present in the second anneal (the sample had only previously been pulsed to 45 K) could effect the temperature dependence of the constant during the second run.

Figure 16 shows the annealing results found at temperature for C_{44} after the first low temperature irradiation. The lower curve represents the values determined from measurements taken at each of the pulse temperatures near the end of the 15 minute pulse. The middle and upper curves follow the data taken after the crystal had already been pulsed to 45 K and 60 K

Fig. 15. The difference between the resonant frequency before and after thermal neutron irradiation which was measured at several temperatures for the two C_{11} runs. The results from both runs have been normalized to the same defect concentration ($\Delta\rho=0.435\times10^{-3}$ μ-Ω-cm).

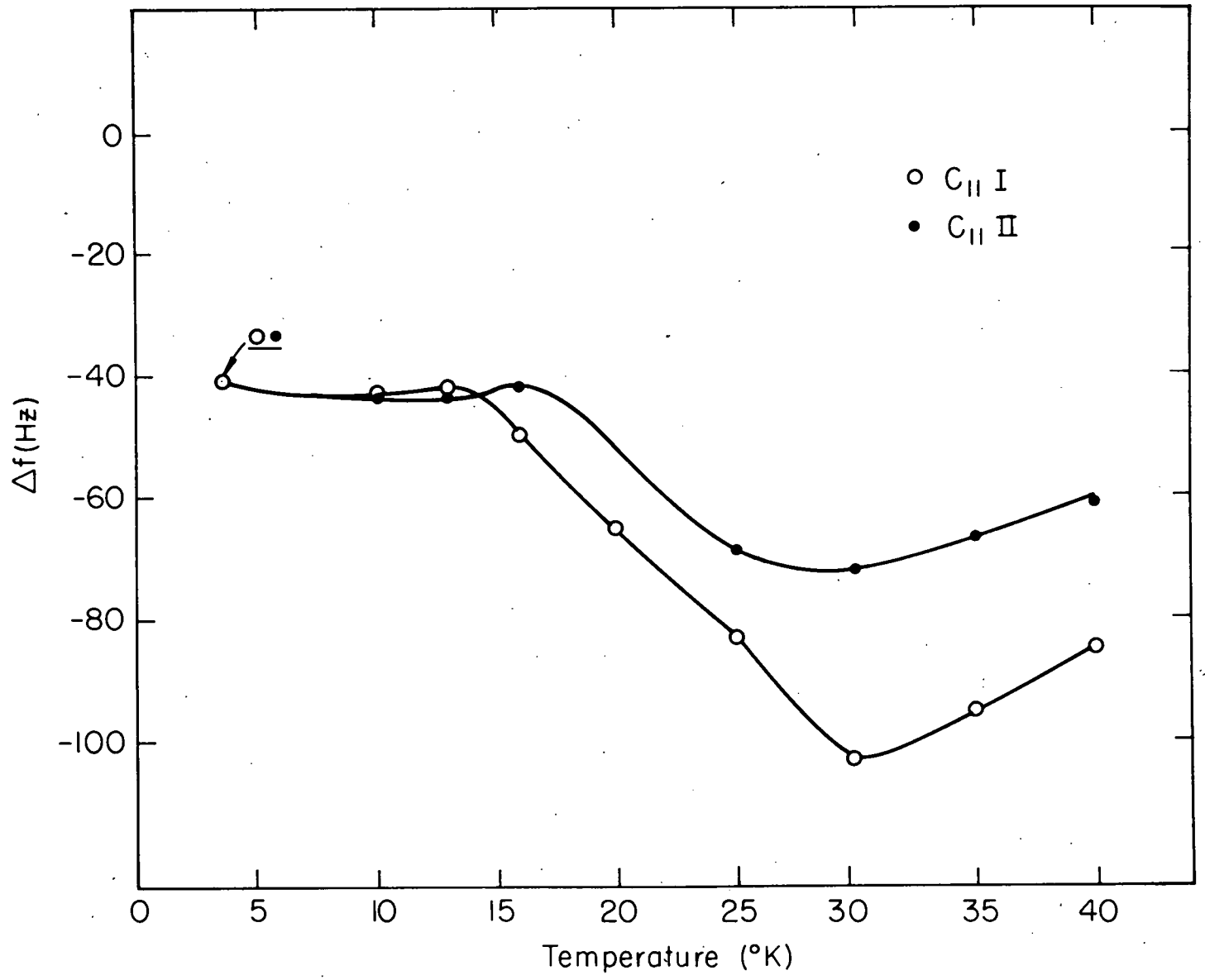
0
-20
-40
-60
-80
-100
Δf(Hz)
0
5
10
15
20
25
30
35
40
Temperature (°K)
○ C|| I
● C|| II

Fig. 16. The difference between the resonant frequency before and after thermal neutron irradiation which was measured at several temperatures for the first C_{44} run. The lower curve represents the values determined from measurements taken at each of the pulse temperatures near the end of the 15 minute pulse. The middle and upper curves follow the results obtained after the crystal had already been annealed to 45 and 60 K respectively.

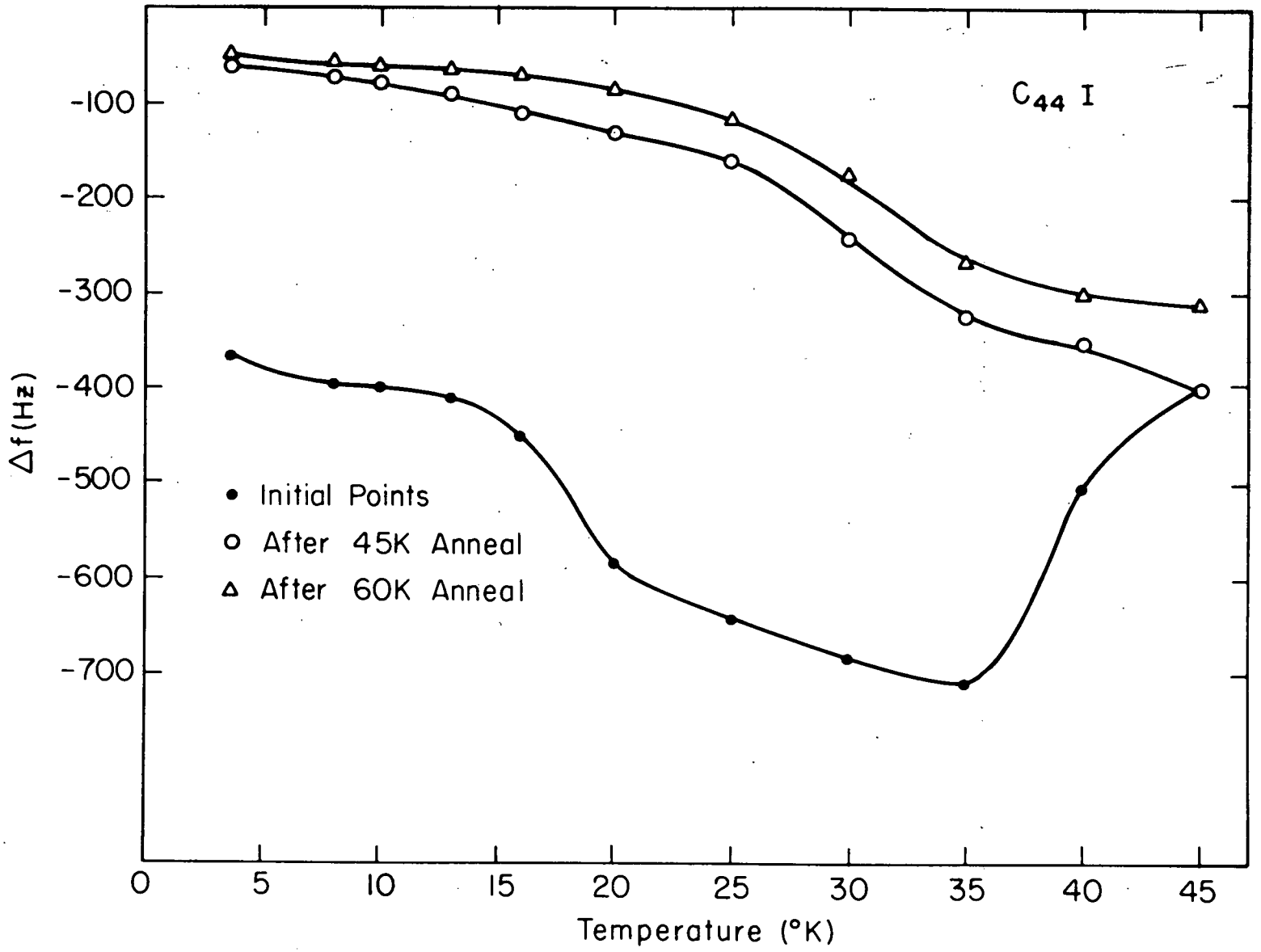
C_{44} I
-100
-200
-300
-400
-500
-600
-700
Δf (Hz)
• Initial Points
o After 45K Anneal
Δ After 60K Anneal
0
5
10
15
20
25
30
35
40
45
Temperature (°K)

Fig. 17. The difference between the resonant frequency before and after thermal neutron irradiation which was measured at several temperatures for the second C_{44} run. The lower curve represents the values determined from measurements taken at each of the pulse temperatures near the end of the 15 minute pulse. The upper curve follows the results obtained after the crystal had already been pulsed to 35 K.

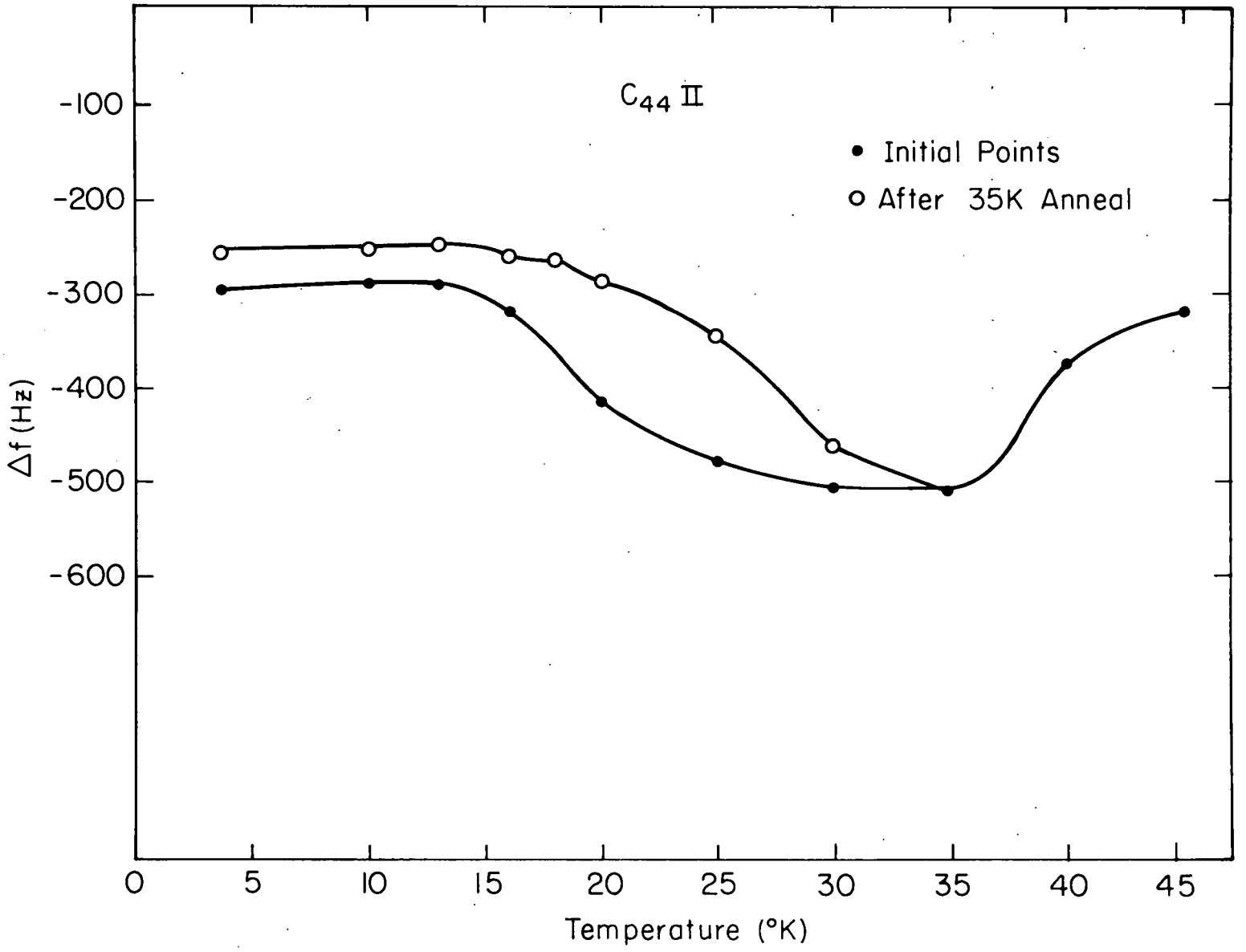
C_{44} II
• Initial Points
o After 35K Anneal
-100
-200
-300
-400
-500
-600
Δf (Hz)
0
5
10
15
20
25
30
35
40
45
Temperature (°K)

Fig. 18. The difference between the temperature dependence of the C' resonant frequency before and after thermal neutron irradiation, during various stages of the annealing program.

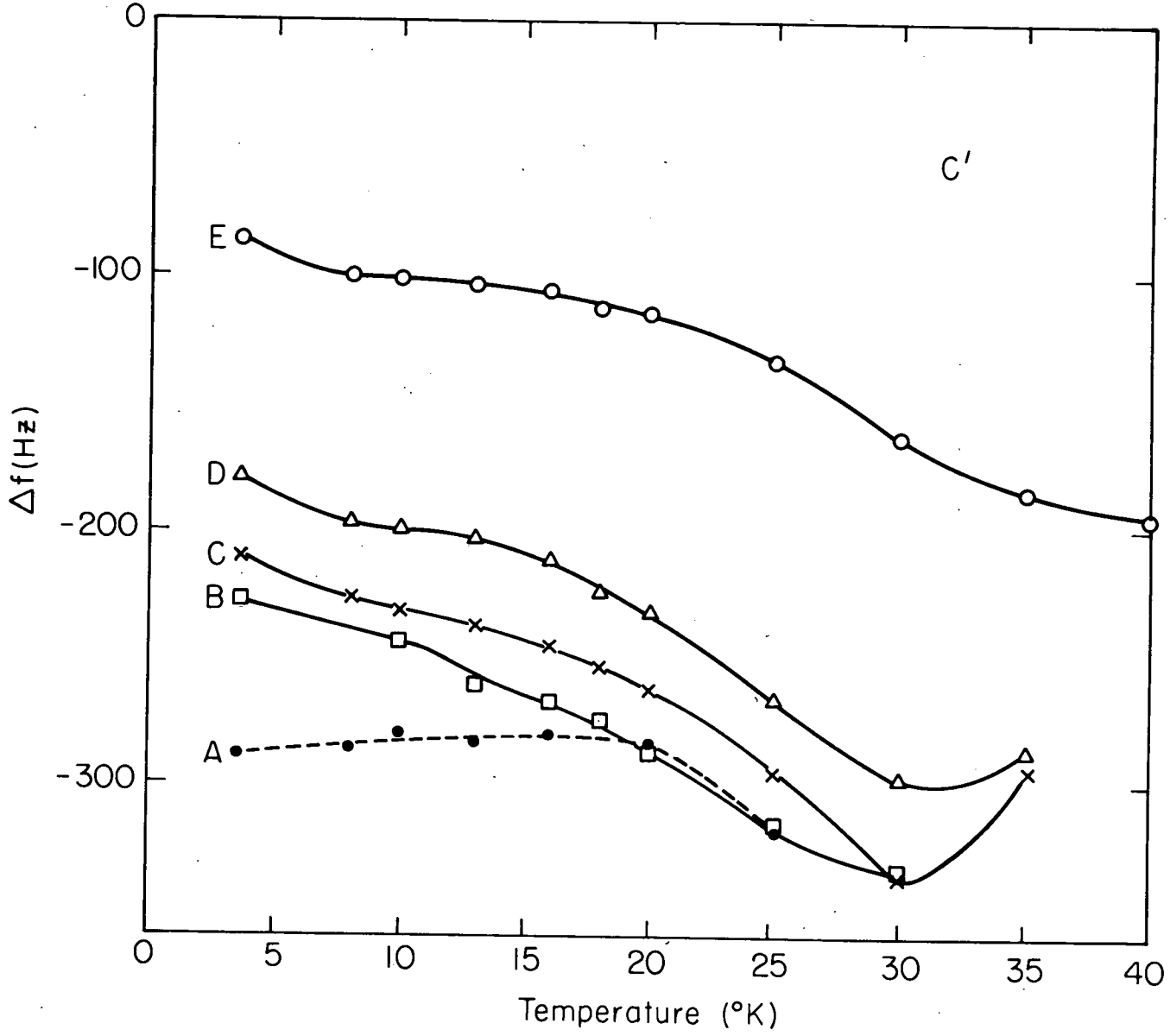
0
-100
-200
-300
Δf(Hz)
C′
E
D
C
B
A
0
5
10
15
20
25
30
35
40
Temperature (°K)

respectively. A sharp dispersion is quite evident near 18 K, which has disappeared by the time the middle and upper curves were obtained. Also, a much broader relaxation around 30 K is apparent in both these latter two curves.

The results obtained during the annealing of C_{44} after its second irradiation are shown in Fig. 17. Here, the points of the upper curve follow data taken subsequent to a 35 K pulse. It appears from this figure that the 18 K relaxation has not completely annealed by 35 K. In contrast to C_{11}, these two different runs are in very good quantitative agreement. (None of the four factors which were mentioned above as possible explanations for the lack of quantitative agreement in the two C_{11} runs were present in either the C_{44} or C' experiments.)

Measurements for the C' mode are presented in Fig. 18. A much more detailed annealing program was undertaken with this sample. Pulses were first made, and readings taken, at the indicated temperatures (curve A) up to and including 25 K. Measurements were then performed at all temperatures indicated by the points of curve B. After a hold at 30 K for 15 minutes the sample was returned to the reference point, and the temperature region to 35 K was traversed in a similar fashion. These results are represented by curve C and the corresponding results after the anneal to 35 K are represented by curve D. Then the crystal was pulsed to 40 K, and finally 45 K. Subsequent to the 45° pulse, all points were then sampled again, and these are represented by curve E.

No evidence of the sharp dispersion at 18 K which occurred in the C_{44} runs is evident in these results, although the broad dispersion around 30 K is again present.

IV. DISCUSSION

A. Effects Observed at Liquid Helium Temperatures

It is clear from Table 1 that no extremely large effects ($d\ln C/dY = -100$) were found in any of the elastic constants during irradiation; the magnitudes of the effect for all three constants lie intermediate in the range of previously reported values. However, the two shear constants do exhibit a significantly larger effect than the longitudinal constant. Furthermore, the relative change in the bulk modulus during irradiation, which can be calculated from the present results, is an order of magnitude smaller ($d\ln B/dY = -2$) than either of the changes observed in the two shear modes. Therefore some consideration must be given to the particular constant which was measured when comparing different studies of irradiation induced elastic constant changes.

Although all possible second order constant changes can be determined from those found in the complete set of independent constants measured here, the previously reported values were all measurements using one of the above constants or Young's modulus, Y. The magnitude of Young's modulus varies for deformations in different directions. The magnitude of the irradiation effect, $d\ln Y/dY$, calculated on the basis of the present results also varies in the same manner, from a maximum value of -17 for deformation in a $\langle 100 \rangle$ direction to -14 for a $\langle 111 \rangle$ direction. Since these values fall within the range reported above, the wide spread in the previously reported results cannot be understood in terms of variations in behavior of the different elastic constants.

The annealing curves shown in Fig. 12 indicate quite clearly that the irradiation induced changes in the three different constants do not

recover in the same fashion. Moreover, these results also show that the recovery of any particular constant is different in different temperature regions. Since these temperature regions each involve the annealing of different kinds of defects, the amount of irradiation produced change in any given constant depends upon the kinds of defects which are generated. It is important, therefore, to associate the elastic modulus recovery stages with the appropriate defect recovery stages characteristic of resistivity recovery.

Because only the general features of stage I annealing may be determined from the present resistivity measurements, we use the results from other more detailed investigations of this annealing region. However, we must first correct for the differences in annealing rate between these investigations and the present set of experiments. For stages I_A-I_D the results obtained from three different studies[2,40,41] agree within ± 1 degree K when corrected[42] to the present annealing rate. The value of the temperature where the maximum rate of annealing of each stage occurs is: I_A = 16 K, I_B = 27 K, I_C = 32 K, and I_D = 41 K. The dose dependence of I_E makes it more difficult to locate accurately. From studies of slow neutron[20] and low energy electron damage[41] in which defect concentrations comparable to those introduced by the present irradiations were used, we estimate that I_E annealing should occur between 45 and 55 K in the present experiments.

For further simplification of the discussion, the annealing results of Fig. 12 are replotted in Fig. 19 as the percentage of the total irradiation produced frequency change which remains at various stages of the annealing program. The temperatures corresponding to the centers of the various stages determined in the manner discussed above, as well as a curve representing the average of the present resistivity data are included in this

Fig. 19. The percentage of the total irradiation produced frequency change measured at 3.6 K which remains at various stages of the annealing program for all three modes. A curve representing the average of the resistivity data is also shown. The temperatures corresponding to the maximum rate of annealing of the substages, which were determined in the manner discussed in the text, have been marked on the abscissa.

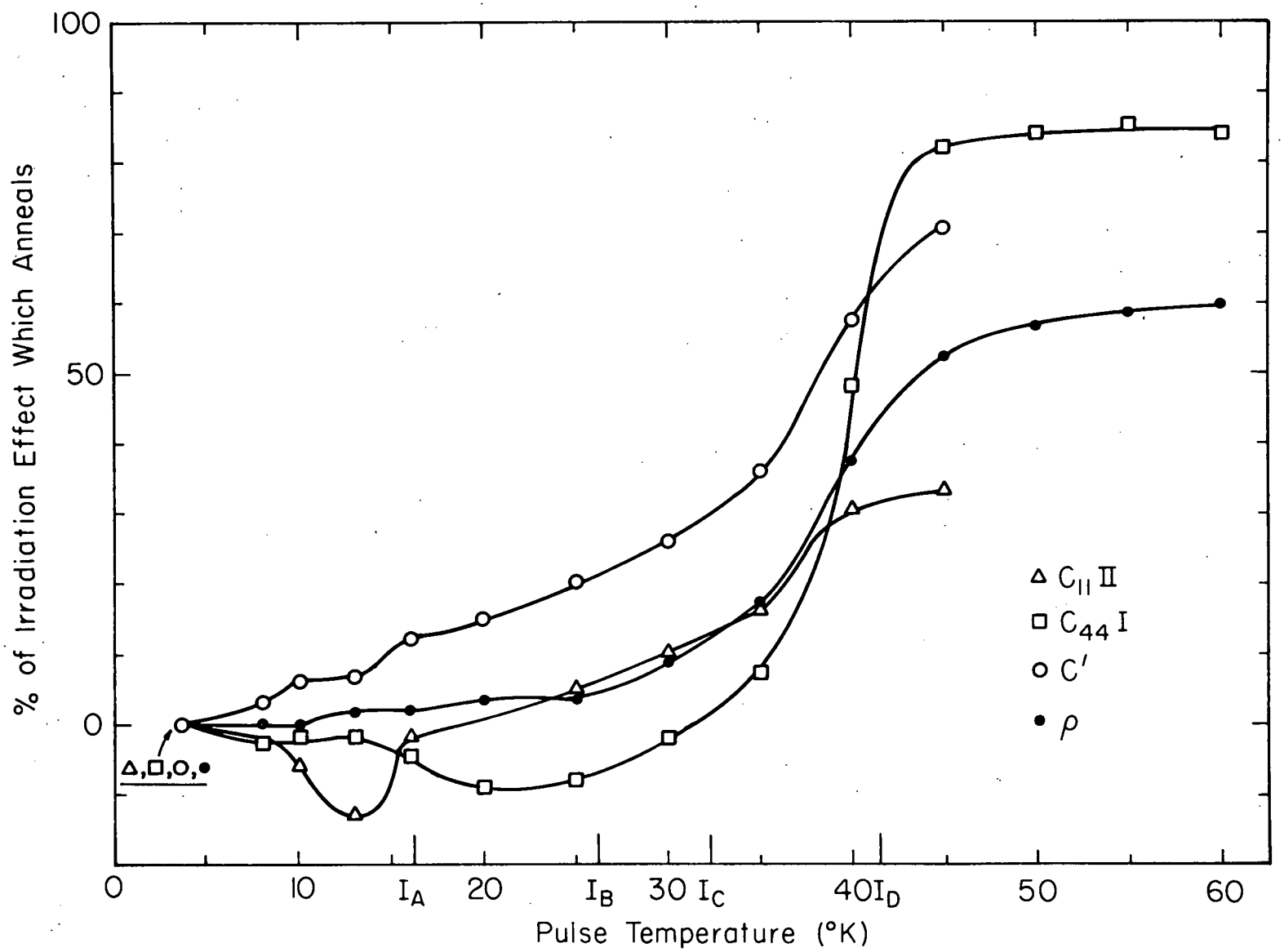
100
50
0
% of Irradiation Effect Which Anneals
△,□,○,●
0
10
I_A
20
I_B
30
I_C
40
I_D
50
60
Pulse Temperature (°K)
△ C_{11} II
□ C_{44} I
○ C′
● ρ

figure. These results indicate that the annealing of the effects for all the measured constants can be roughly divided into three different temperature regions of distinctly different behavior.

In the recovery range from 3.6 K to a few degrees beyond the I_A peak (to about 20 K), all three modes change significantly more than would be expected on the basis of resistivity studies. Furthermore, both the C_{11} and C_{44} constants experience an additional decrease of about 10%. Such an effect could be explained by the thermal conversion of defects, or else by the recovery of damage which gives a positive contribution to the modulus change. For pulse temperatures in the range where the I_B and I_C close pairs recover (between approximately 20 and 37 K), all three modes anneal in a similar fashion and all in the same manner as the resistivity. Above 37 K (the onset of I_D), the annealing behavior is quite different for the three constants, and only C' recovers as the resistivity. More than two-thirds of the relative change in C_{44} introduced during irradiation anneals in this latter temperature interval, in contrast to only about one-sixth of that in C_{11}. Approximately one-third of the irradiation produced increase in resistivity recovers in this range.

It is apparent from the annealing results presented in Fig. 19 that not only does the irradiation induced effect vary among the different elastic constants, but the effect on any particular constant is also dependent upon the kinds of defects present in the lattice. Thus the amount of modulus change produced by an irradiation cannot be directly related to an incremental change in resistivity without regard to both the particular constant being measured and the type of damage which is created. For this reason, modulus changes produced with different irradiation particles or with irradiation at

different temperatures would not be expected to scale in exactly the same manner as the measured resistivity changes.

Most of the theoretical work in this field has been concerned with the contribution to the elastic constants from isolated vacancies and interstitials. The total irradiation produced changes include the effects of close pairs as well as more complex types of defects, so they are not convenient for comparison with theory. Therefore a method is needed for separating out the effects of free interstitials and vacancies. Since stage I_D is generally believed to arise from the recombination of interstitials with their own vacancies (the two defects being sufficiently separated that their mutual interaction can be considered negligible), the ratio of the amount of elastic constant recovery to that of the resistivity in stage I_D provides a direct means for determining the magnitude of this effect. The results for $d\ln C/d\gamma$ obtained by using the I_D annealing in the present experiments (taken to occur between 35 K and 45 K), are given in Table 2.

Table 2

The contributions from I_D defects to the measured set of elastic constants

Run	$\frac{d\ln C}{d\gamma}$
C_{11} II	-2
C'	-15
C_{44} I	-29
C_{44} II	-33

It would likewise seem possible to estimate the free interstitial contribution by using the changes observed during the annealing of stage I_E. However, the relatively small amount of I_E recovery which occurs, coupled

with the aggregation and trapping of defects during the long range migration of the interstitial, makes interpretation more difficult. The present results which are available only for C_{44} I, indicate that the effect ($d\ln C_{44}/d\gamma$) from the I_E defect is only about -8. An accurate determination of the relationship between the recovery of the elastic constants and resistivity changes in stage I_E must await more detailed experimental results, preferably from studies of small defect concentrations created by low-energy electron irradiation.

The annealing behavior of the bulk modulus is completely different from that of all the other constants. Since a hydrostatic stress does not alter the configuration of the defects in a cubic lattice, the bulk modulus change should be free of relaxation and polarization effects, and thus provides the most direct measurement of the bulk effect. As mentioned previously, the change in the bulk modulus during irradiation, $d\ln B/d\gamma$, is only -2. Most surprisingly, this effect exhibits no significant recovery during the annealing through 45 K. In particular, no measureable change in the irradiation induced bulk modulus effect occurs during stage I_D, where more than one-third of the resistivity damage anneals. Thus it appears that the bulk effect from separated vacancies and interstitials is very small, and not even the sign of this contribution is evident from the present, or any previous experiments.

This small effect could be a result of small contributions from both vacancies and interstitials, or else the consequence of nearly equal and opposite magnitudes. This indication of a small magnitude (< 1) for the bulk effect is in agreement with the range of reported theoretical estimates (-10 to +10).

If the bulk effect is indeed so small, the large decreases shown in Table 2 must be a result of other types of contributions, such as polarization effects. In fact, this pattern of elastic constant changes is just that expected on the basis of a recent calculation by Dederichs[43] of the polarizability of the ⟨100⟩-split, dumbbell interstitial.

Polarizability effects may occur when the defect symmetry differs from that of the host lattice. In this case, the atoms associated with the defect are no longer sitting at perfect crystal lattice sites. Therefore, when a homogeneous external stress is applied, the defect atoms are displaced by an additional amount relative to the homogeneously deformed lattice.[44] This additional internal strain will cause a decrease in the measured elastic constant; the magnitude of the strain will be determined by the effective force constants in the immediate vicinity of the defect. Dederich's calculation indicates that certain of the force constants for the ⟨100⟩-split dumbbell interstitial allow large internal displacements, with consequently large decreases in certain of the elastic constants. In particular, he estimates the magnitude of the effect to be the largest in C_{44}, less in C' and almost negligible in C_{11}. We see that this pattern is clearly obeyed by the present results. A quantitative comparison must await the publication of the details of the calculation.

The attenuation decrease which was observed in C_{11} and C' during irradiation is in agreement with the expected reduction of the electron-phonon contribution to the attenuation. This reduction arises from a decrease in the electron mean free path due to the additional scattering centers created by the irradiation. Electronic attenuation is discussed in detail by Pippard[45] and Mason,[46] who use a free electron approximation to calculate

the magnitude of attenuation, $\alpha(\frac{\text{nepers}}{\text{cm}})$, to be expected per resistivity increment, ρ. The results are different for longitudinal (L) and shear (S) modes, and depend upon the frequency, f, and velocity, v, of the sound wave as well as the density, ρ_d, of the sample:

$$\alpha_L = \frac{2f^2}{15\rho_d v_L^3} \left(\frac{h^2(3\pi^2 N)^{2/3}}{e^2 \rho} \right) \tag{5}$$

$$\alpha_S = \frac{3}{4}\left(\frac{v_L}{v_S}\right)^3 \alpha_L \, . \tag{6}$$

N is the number of electrons per unit volume and e is the charge carried by one electron.

A comparison of the experimental results with the values obtained from these equations is made in Table 3, and the agreement is considered good.

Table 3

A comparison of the theoretical and experimental results for the change in electronic attenuation due to the irradiation produced resistivity change

Mode	Theoretical α (db/μ-sec)	Experimental α (db/μ-sec)
C_{11}	-0.0050	-0.0061
C'	-0.046	-0.031

The theoretical estimate for C_{44} indicates that it is smaller than the experimental uncertainty of the present measurements, and is consistent with the fact that no systematic change of attenuation was observed in either of the two C_{44} runs. This theory also accounts for the observed agreement between the attenuation and resistivity recovery during annealing (Fig. 13).

This is believed to be the first such measurement of the change in electronic attenuation produced by irradiation. The results indicate that

attenuation measurements can provide a reliable measurement of defect concentrations in the same sample in which elastic constant changes are measured. This is a very useful technique, especially for megahertz elasticity measurements where sample dimensions are too large for ordinary resistivity measurements to be made.

B. Effects Observed above Liquid Helium Temperatures

1. General Formalism

The normal temperature dependence of elastic constants is a consequence of the anharmonic nature of the lattice phonon interactions and a complete description is not within the intent of the thesis. However, since an understanding of this dependence is helpful in interpreting the irradiation induced temperature dependent effects, a brief outline of the general approach[23] for calculating the temperature dependence of elastic constants will be given here.

The thermodynamic definition of the N'th order isothermal elastic constants, $C^{T}_{ijk\ell\cdots}$, in terms of the strain derivatives, $\frac{\partial}{\partial \eta_{ij}}$, of the free energy, F, and volume, V, is:

$$C_{ijk\ell\cdots} \equiv \frac{1}{V} \left. \frac{\partial^N F}{\partial \eta_{ij} \partial \eta_{k\ell\cdots}} \right|_T \quad . \tag{7}$$

The free energy may be written as the sum of the cohesive energy, Φ, the total vibrational energy from the phonon modes, α, and an entropy term, -TS:

$$F = \Phi + \sum_{\alpha} \epsilon_{\alpha} - TS \quad . \tag{8}$$

Here $\epsilon_{\alpha} = \frac{\hbar\omega_{\alpha}}{e^{\frac{\hbar\omega_{\alpha}}{kT}} - 1}$. Defining the state of zero stress as the absence

of all vibrations, the expression for the isothermal second order elastic constants to first order in the vibrational part of the strain, η, is then given by:

$$C^{T}_{ijk\ell} = \tilde{C}^{o}_{ijk\ell} + \frac{1}{V^{o}} \sum_{\alpha=1}^{3N} \left[\frac{1}{\omega_{\alpha}{}^{o}} \frac{\partial^2 \omega_{\alpha}{}^{o}}{\partial \eta_{ij} \partial \eta_{k\ell}} \epsilon_{\alpha}{}^{o} - \frac{1}{\omega_{\alpha}{}^{o2}} \left(\frac{\partial \omega_{\alpha}{}^{o}}{\partial \eta_{ij}} \right) \left(\frac{\partial \omega_{\alpha}{}^{o}}{\partial \eta_{k\ell}} \right) C_{\alpha}{}^{o\ T} \right]$$

$$+ \eta (\tilde{C}^{o}_{ijk\ell} + \tilde{C}^{o}_{ijk\ell mm}) \ . \qquad (9)$$

The angular frequencies $\omega_{\alpha}{}^{o}$ are the frequencies of oscillation about the static lattice; $C_{\alpha}{}^{o}$ represents the Einstein heat capacity for mode α and the $\tilde{C}^{o}_{ijk\ell\cdots}$ are the static lattice elastic constants.

This general expression applies to both perfect and imperfect lattices, and gives the temperature dependence of the elastic constants if the phonon frequencies and their strain derivatives are known. Conversely, it can be used to gain information about the frequencies if the temperature dependence of the elastic constants is available. The principal concern of the present discussion is the effects produced by point defects, but we first will consider briefly a comparison of the present results obtained prior to the thermal neutron irradiations, with a recent perfect crystal calculation by Garber and Granato.[23] This comparison is important because the very precise and demonstrably dislocation-insensitive data provide the best known experimental check presently available for the theory.

Garber and Granato calculated the temperature dependence of the elastic constants from Eq. (9), by assuming the strain dependence of all the phonon frequencies is the same as that in the low temperature, long wavelength region where the derivatives can be calculated on the basis of elasticity theory. In this manner, they find an expression for the temperature dependence of the elastic constants in terms of third and fourth order

constants. Since short range repulsive interactions should be increasingly more important for the higher order constants, they further assume that only nearest neighbor interactions will be significant in determining the fourth order constants. Thus they were able to reduce the final expressions to ones containing only measured third order constants and one fourth order constant. These final expressions for the temperature dependence of the second order elastic constants of copper for low temperatures in terms of the fourth order constant C_{1111} (10^{10}dynes/cm^2), in units of (10^2 dynes/cm^2 K^4), are:

$$(C_{11}(T)-C_{11}(T=0))/T^4 = -(5.46\times10^{-4})C_{1111} + 10.1 \quad (10)$$

$$(C_{44}(T)-C_{44}(T=0))/T^4 = -(2.73\times10^{-4})C_{1111} + 5.43 \quad (11)$$

$$(C'_{(T)} - C'_{(T=0)}) /T^4 = -(1.36\times10^{-4})C_{1111} + 3.76 \; . \quad (12)$$

Three independent determinations of C_{1111} can be made by fitting these equations to the experimental results presented in Fig. 14. The values obtained in this manner are given in Table 4; the length change correction given in Eq. (4) is less than 5% in this case, and has been neglected. Also shown in

Table 4

A comparison of the calculations of Garber and Granato[23] with the present results of the pre-irradiation temperature dependence.

Mode	Present Results C_{1111}(10^{14} dyn/cm^2)	Garber and Granato C_{1111}(10^{14} dyn/cm^2)
C_{11}	1.2	1.05
C_{44}	.7	0.87
C'	1.3	1.07

the table are corresponding results found by Garber and Granato by fitting the high temperature portion of their theory to other available data.

The three different values of C_{1111} obtained in both the high and low temperature regions are reasonably consistent with each other in consideration of the crude assumption of a single fourth order constant. This agreement is in contrast to a discrepancy of more than a factor of two obtained with the only other previously available measurement sensitive enough to allow a comparison. The previous measurements were made by Alers et al.[39] for the C_{44} mode of copper from 4 to 21 K, but no procedure was used to check possible dislocation contributions. Such contributions would be expected to destroy such agreement, since dislocation effects may be strongly temperature dependent.

2. The Temperature Dependence of the Defect Contributions to the Elastic Constants

Following thermal neutron irradiation, strong changes were observed in the temperature dependence of all three elastic constants. The most pronounced change occurs in the C_{44} results (Fig. 16), and includes in part a sharp drop in resonant frequency near 18 K. This temperature dependence is in qualitative agreement with the relaxation effect which was anticipated prior to the actual experiment. However, it is important to realize that the lower curve in Fig. 16 contains contributions from at least two other sources besides the observed relaxation: (1) some annealing of defects occurs at each temperature and (2) the defects which remain after the 45 K annealing pulse also give a temperature dependent effect.

In order to obtain a more quantitative picture of the anelastic process, we first correct each point of the lower curve in Fig. 16 for the annealing which was measured at 3.6 K. The magnitude of this correction is evident from a comparison of the corrected and original curves shown in

Fig. 20. In particular, this annealing correction has practically no effect on the sharp dispersion near 18 K. The temperature dependence from the defects which remain after the 45 K annealing pulse is given by the upper curve in Fig. 16. Consequently, we can remove this contribution by considering only the difference between the upper curve of Fig. 16 and the corrected curve of Fig. 20. This difference represents the behavior of the irradiation induced temperature dependence of the C_{44} elastic constant during the annealing from 3.6 to 45 K, and is presented in Fig. 21.

This behavior indicates that a defect is created during the irradiation which introduces a sharp relaxation modulus effect centered about 18 K and which anneals over the temperature interval from 25 to 40 K. Although a curve obtained by treating the data of C' in a similar fashion also gives evidence of temperature dependent effects, the dependence is considerably weaker and no indication of a drop near 18 K is present. It is not possible to obtain a similar curve from the C_{11} results because of the different annealing program which was followed.

As mentioned in section I, this effect has been observed previously by Nielsen and Townsend (NT),[9] who attributed it to the stress induced ordering of the interstitial member of either the I_B or I_C defect. Their observation that the effect occurs in the Young's modulus of a ⟨111⟩-oriented single-crystal and not in a ⟨100⟩-oriented single-crystal agrees with the present results, which show the modulus defect occurs in the C_{44} and not the C' mode.

By combining the present 10 MHz results with the kHz measurements of NT, we can reach more quantitative conclusions than are available from each study taken independently. For example, the measurement of the anelastic

Fig. 20. A comparison of the results for the irradiation produced change in the resonant frequency observed at the various pulse temperatures during the first C_{44} run, with the same results corrected for the annealing measured at 3.6 K.

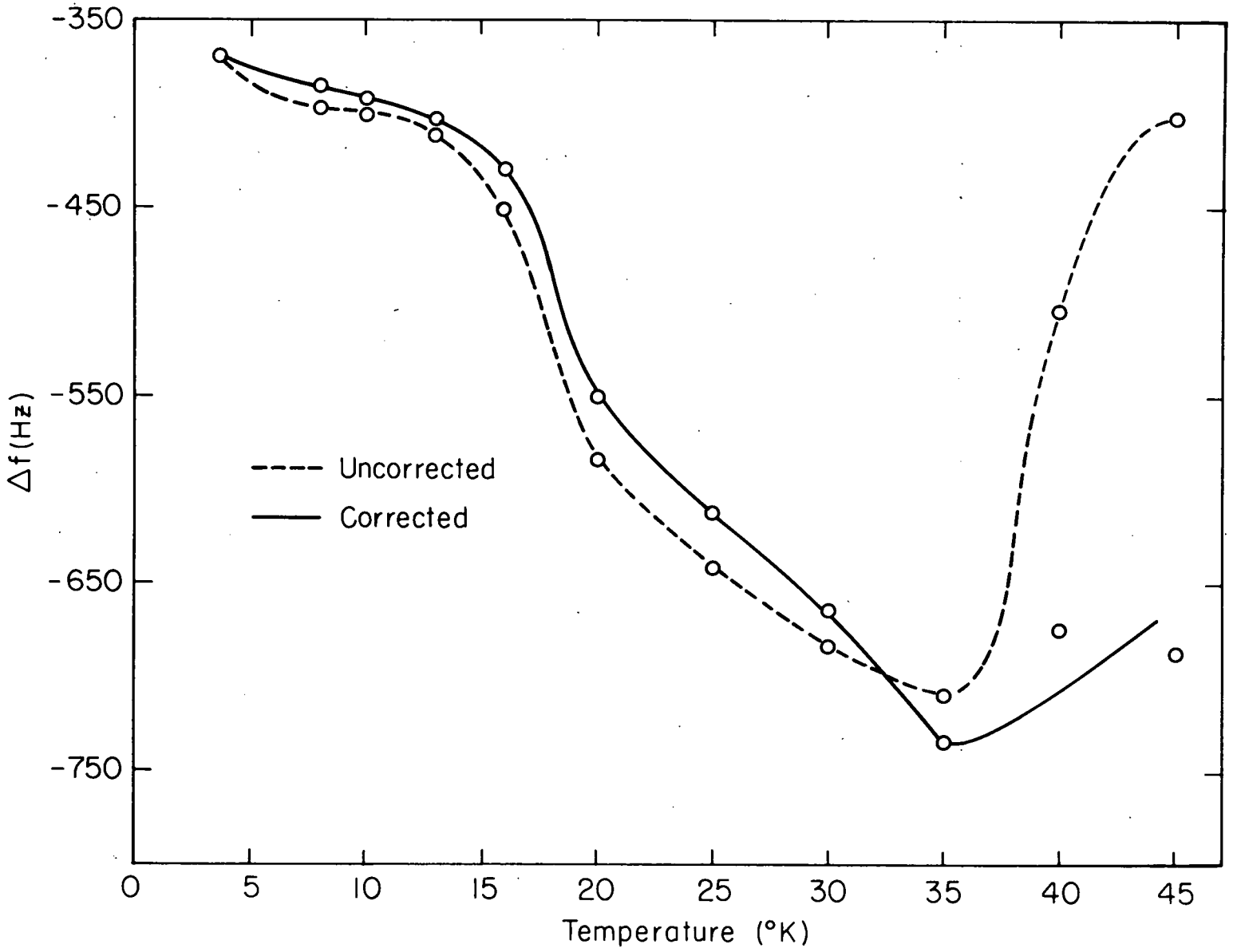
-350
-450
-550
-650
-750
Δf(Hz)
Uncorrected
Corrected
0
5
10
15
20
25
30
35
40
45
Temperature (°K)

Fig. 21. The behavior of the irradiation induced temperature dependence of the C_{44} resonant frequency during the annealing from 3.6 to 45 K.

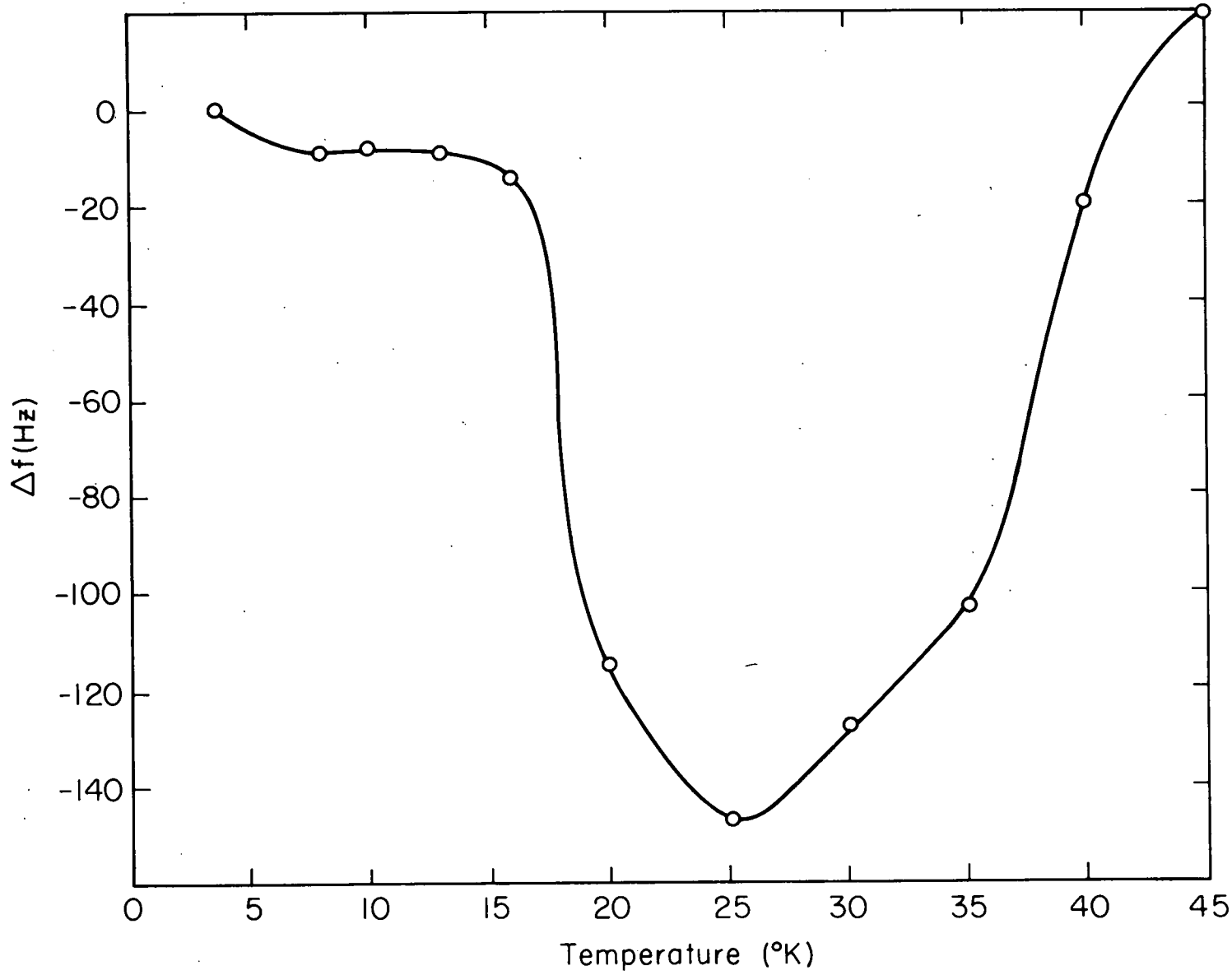
0
-20
-40
-60
-80
-100
-120
-140
Δf(Hz)
0
5
10
15
20
25
30
35
40
45
Temperature (°K)

contribution at two very different frequencies provides a good estimate of the attempt frequency. This frequency was determined to be $6\pm2\times10^{11}$ Hz; the value of the energy of activation is then $0.017\pm.002$ eV. These values are in good agreement with those reported solely on the basis of the NT experiments: $8\times10^{11\pm1}$ Hz for the attempt frequency and $0.015\pm.002$ eV for the energy of activation.

As shown in Fig. 21, the anelastic effect anneals between temperatures of approximately 25 and 40 K, in agreement with NT. Since NT were able to observe this annealing in detail, it is possible to analyze which of the annealing substages should be associated with the recovery of the anelastic process.

Although this annealing range is broad enough to include both the I_B and I_C stages, we note that in the present results the center of this annealing range lies within one degree of the I_C resistivity peak and more than 5 degrees above that of I_B. In order to determine where stages I_B and I_C occur in the NT study, we again correct the data of various authors[2,41,42] for the difference in annealing rate.[40] These results are given in Table 5.

Table 5

The location of the maximum rate of annealing of stages I_B and I_C as determined by various investigators, and their predicted occurrence in the NT experiment based on the annealing rate correction of Nilan and Granato.[40]

Author	I_B		I_C	
	Observed	Corrected	Observed	Corrected
Nilan and Granato[41]	29.6	27.7	34.5	32.3
CSW[2]	26.25	26.7	31.25	31.8
Snead et al.[42]	26.5	27.9	30.5	32.3
Average		27.4		32.1

We note that the annealing peak of the I_C defect given in Table 5 coincides almost exactly with the value of 32 K reported by NT for the maximum rate of recovery of the anelastic process. Furthermore, the annealing of the anelastic process does not begin (26 K) until after the onset of I_B recovery. For these reasons, we conclude that I_C is the only recovery stage with which this relaxation may be identified.

Many attempts have been made to assign a particular lattice configuration to each of the three close pair defects solely on the basis of their relative activation energies, but this approach leads to a wide variety of possible choices. However, the determination of the symmetry of a relaxation from the I_C defect places further restrictions on these choices, and makes a new attempt more promising.

Relaxation can occur when an applied stress causes certain of the defect orientations which were equivalent in the unstressed crystal to become energetically favored. In a cubic crystal, if the defect symmetry axis lies along one of the symmetry directions, ⟨100⟩, ⟨110⟩ or ⟨111⟩, then the absence of a relaxation in the C' mode indicates trigonal symmetry. The assignment of the strain symmetry axis of the defect along a ⟨111⟩ direction by NT[9] is consistent with this interpretation.

For isolated defects, the symmetry axis would be expected to lie along one of the symmetry axes of the crystal. However, for a close pair defect the symmetry axis need not lie along one of the symmetry directions. In this case, the defect orientations whose relative energies are unaffected by a direct measurement of the C' elastic constant are those in which the two orientations are symmetric about a (100) plane. Therefore, the type of motion which is compatible with the relaxation observed in the present case

must possess mirror symmetry about a (100) plane. Since the two orientations should be equivalent in the unstressed crystal, the vacancy member of the close pair must also lie in the same (100) plane.

Additional information regarding the nature of the defect is provided by the magnitude of the anelastic effect. The anelastic behavior of point defects is often discussed in terms of an elastic dipole,[47] since in many ways the effect is similar to that experienced by an electric dipole under the influence of an applied field. The second rank tensor, λ_{ij}, used to describe the elastic dipole is the strain component per unit mole fraction of defects:

$$\lambda_{ij} \equiv \frac{\partial \epsilon_{ij}}{\partial C_p} .$$

For trigonal defects in cubic materials, there are only two independent elements of this tensor, λ_1 and λ_2, and only the absolute value of the difference between these two, the so called "shape factor" $|\lambda_1-\lambda_2|$, can be obtained from measurements of the elastic moduli. This difference may be found from the relation[47]:

$$\frac{1}{3}\frac{\Delta C_{44}}{(C_{44})^2} = \frac{4}{27}\left(\frac{C_0 V_0}{kT}\right)(\lambda_1-\lambda_2)^2 \qquad (13)$$

where C_0 represents the molar concentration of defects and V_0 is the molecular volume.

A review of the energy dependence of the total recovery of close pairs by W. Schilling[48] indicates that about 8% of the total damage in the present experiment is comprised of I_C defects. Using this result and the change of 135 Hz in the resonant frequency indicated in Fig. 21, Eq. (13) gives a value of 0.5 for $|\lambda_1-\lambda_2|$. From the NT results, we also calculate a

value of 0.5. This shape factor implies a difference of approximately 50% in the strain per unit concentration of defects in two principal directions.

The criteria then which must be satisfied for the I_C defect are: (1) it must have a low activation energy for annealing and (2) an even lower activation energy for relaxation; (3) the relaxation must involve motion symmetric about a (100) plane; (4) the vacancy member of the close pair must lie in the same (100) plane; (5) the relaxation must be induced by a measurement of the C_{44} elastic constant and (6) it must be characterized by a relatively large relaxation strength.

Defects whose symmetry strain axes lie along the ⟨111⟩ crystal directions possess trigonal symmetry, and satisfy criteria 3, 4 and 5. If we begin by considering the two interstitial types which appear to be the most energetically stable,[49] the ⟨100⟩-split and body centered configurations, then only two arrangements appear to have both a low activation energy for annealing and trigonal symmetry: (A) the body-centered interstitial with a vacancy at one of the unit cell corners and (B) the ⟨100⟩-split dumbbell with a vacancy in the diagonally opposite (⟨111⟩ direction) corner.

However, the identification of either of these schemes with the I_C defect is unlikely. In configuration A, the arrangement of the pair is such that the interstitial and vacancy are next-nearest neighbors; thus only one closer lattice position, nearest neighbor, is available for both the I_A and I_B defects. Although arrangement B appears good from a proximity standpoint (there are at least five closer lattice positions), the requirement that the dumbbell must move two entire lattice spacings, without annealing, and with an activation energy less than 0.02 eV, in order to relax into an equivalent lattice configuration, makes this arrangement highly improbable. In fact, it

appears that any model which requires motion of the center of mass of the interstitial over a distance greater than the nearest neighbor distance cannot satisfy criterion (2).

Consequently, we are led to the conclusion that it is not the entire vacancy-interstitial arrangement which relaxes, but rather only a reorientation (little or no motion of the center of mass) of the interstitial member that occurs. In this case, the symmetry information which is available from the observed relaxation is characteristic of the interstitial motion, and not of the entire close pair.

We first note that the flipping of a ⟨100⟩-split interstitial between different ⟨100⟩ orientations does not involve motion which is symmetric about a (100) plane, and therefore is not compatible with criterion (3). Thus we conclude that the interstitial member of the I_C close pair cannot have the ⟨100⟩-split configuration frequently assumed for the isolated defect.

However, the large relaxation strength calculated above ($|\lambda_1-\lambda_2| = 0.5$) indicates that the interstitial still is characterized by some form of split configuration. In fact, the observed relaxation strength is even greater in magnitude than that estimated for the isolated ⟨100⟩-split configuration ($|\lambda_1-\lambda_2| = .025$,[50] 0.21[51]). This large value is understandable in terms of the nearby vacancy, which probably allows even further elongation of a split configuration interstitial. Therefore, we are looking for a simple reorientation of a split-configuration interstitial that involves motion which is symmetric with respect to the (100) plane containing the vacancy.

We use the results of a computer calculation by Gibson *et al.*[52] as a guide in selecting which of the nearby lattice sites surrounding a vacancy provides a stable location for an interstitial atom. Their results

for a (100) plane containing the vacancy are shown in Fig. 22. All stable positions have been marked with a large cross. Although these calculations are based on the geometry of a ⟨100⟩-split interstitial, we assume that the somewhat different configuration to be considered below can be approximated by these calculations.

Since the defect must possess a low activation energy for annealing (criterion 1), we eliminate all sites further removed from the vacancy than the site labeled 2 (site 3 and beyond). Site 2 lies along a ⟨100⟩ direction from the vacancy. This arrangement makes it unlikely that the interaction between the two members of the close pair would create more than one equivalent orientation for a split interstitial configuration which would be symmetric with respect to a (100) plane. On the contrary, it appears that a split interstitial located here would simply point directly towards the vacancy. However, these objections do not apply to site 1, where a split-interstitial configuration which satisfies all the criteria may be located.

The proposed model for the I_C defect is shown in Fig. 23, with the center of mass of the split configuration interstitial located at site 1 of Fig. 22; the four equivalent positions of the center of mass of the interstitial have been marked with a cross. The equivalent orientation into which the interstitial is believed to relax has been indicated by a dotted outline.

The value of the shape factor required to give the measured modulus change depends upon the orientation of the defect, becoming larger as the interstitial axis moves closer to the (100) plane. Since the value of 0.5 estimated above by assuming a ⟨111⟩ defect orientation is already considerably larger than the theoretical magnitude of the ⟨100⟩-split interstitial, it is unlikely that the interstitial axis shown in Fig. 23 lies much closer to the (100) plane than does the ⟨111⟩ axis.

Fig. 22. The stability of a vacancy and a nearby interstitial in a (100) plane of copper. The vacancy is at the lower left corner. All stable sites have been marked with a large cross.

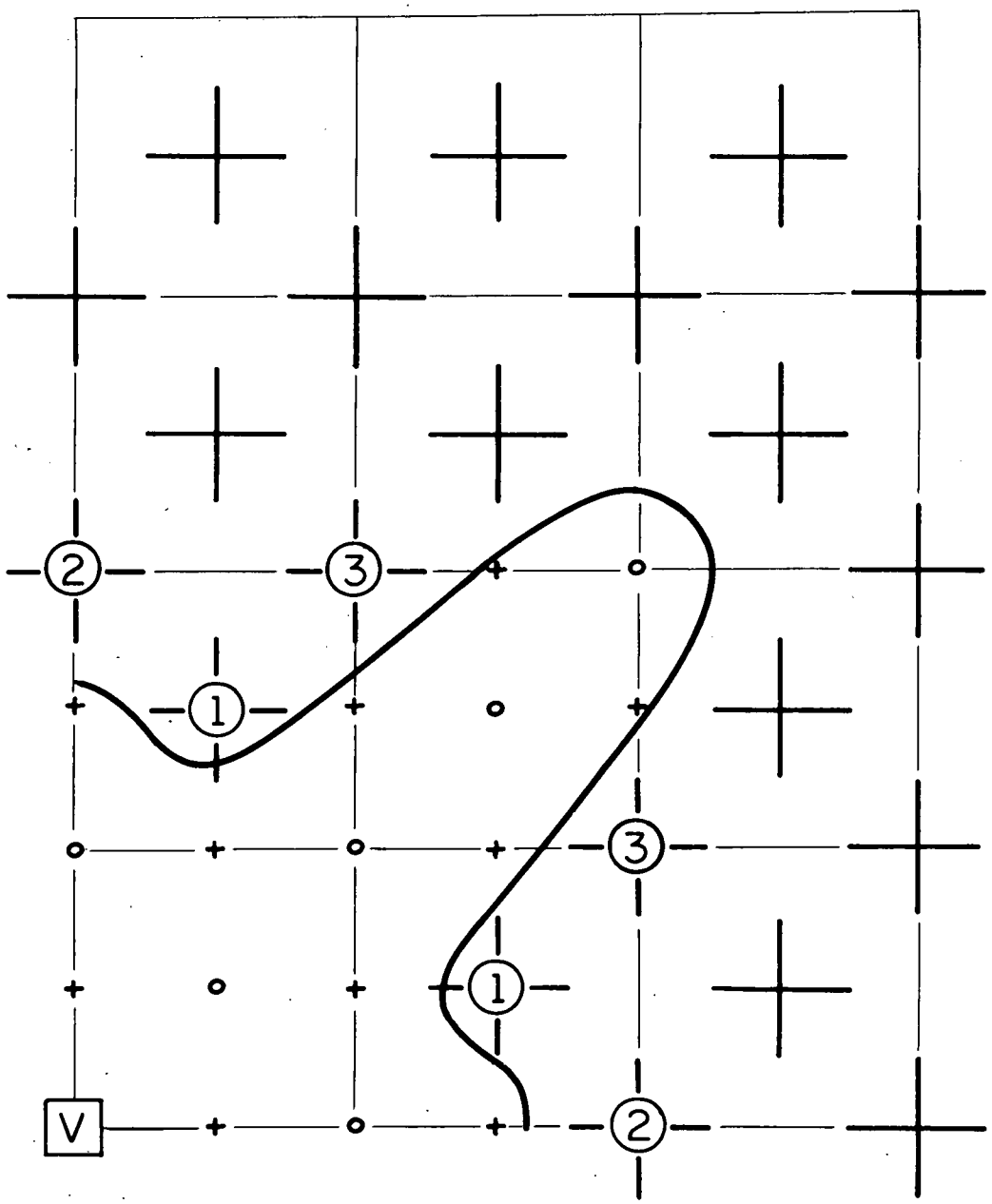
2
3
1
3
1
V
2

Fig. 23. Proposed model for the I_C defect. The four equivalent sites for the center of mass of the interstitial have been marked with a small cross. The equivalent position into which the split-interstitial relaxes is shown by a dotted outline.

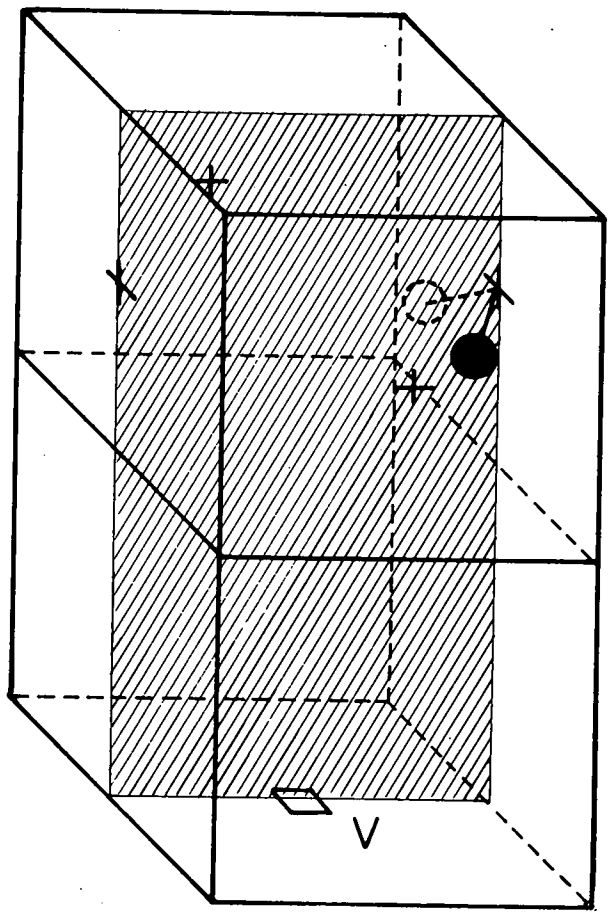
V

The close proximity of the interstitial and vacancy satisfies criterion (1). The proposed relaxation motion is apparently characterized by a low activation energy (2), and is symmetric with respect to a (100) plane containing the vacancy (3 and 4). The relative energies of the two orientations are affected by a direct measurement of the C_{44} elastic constant (5) and due to the split configuration of the interstitial, this relaxation would be expected to give a large relaxation effect (6). Therefore, this model of the I_C close pair satisfies all the criteria discussed above.

The configuration proposed here places the center of mass of the interstitial defect in the same lattice position with respect to the vacancy as the model suggested previously by Peretto et al.[53] Their model was used to explain the observation of a magnetic after-effect for the I_C defect in nickel, and involved the motion of the center of mass of the interstitial between the four equivalent sites marked in Fig. 23. However, the model of Peretto et al.[53] is based on the ⟨100⟩-split interstitial, and is inconsistent with the symmetry requirements imposed by the elastic constant measurements. Furthermore, if the magnetic after-effect does involve motion of the center of mass, the model presented here would allow such motion with apparently only a slightly higher activation energy than that characteristic of the relaxation.

Besides the additional temperature dependence introduced by the I_C relaxation process, further changes in the temperature dependence of all three elastic constants are apparent in Figs. 15-18. We next turn to a discussion of these results.

We first note that the measurements obtained with the C_{44} mode subsequent to a 60 K annealing pulse, and with the C' mode subsequent to a 45 K pulse, indicate that a significant portion of the irradiation induced temperature dependence is due to defects which do not anneal in stage I. Since annealing behavior was not studied above this recovery stage, no analysis of this portion of the effect will be attempted.

We next separate the temperature dependent contributions from particular stage I defects by looking at the change in the temperature dependence of the elastic constants which occurs between appropriate annealing pulses. The difference between the measured temperature dependence after an anneal to temperature T_1, and that measured after an anneal to temperature T_2, gives the elastic constant temperature dependence which is introduced during irradiation by the defects which anneal between T_1 and T_2. The results obtained with the C' mode (Fig. 18) permit separation of the temperature dependent contributions from the I_B, I_C, and I_D defects, since the temperature dependence of the elastic constants of the irradiated samples was measured after anneals to 25, 30, 35, and 45 K. The results from the C_{44} mode (Fig. 16) only allow separation of the contribution from the I_E defects, since measurements were made only after 45 and 60 K anneals. No separation is possible with the limited C_{11} data (Fig. 15).

The change in the temperature dependence of the resonant frequency which occurs during various annealing intervals for the C' mode is given in Table 6. No temperature dependent contribution is evident from the defects which anneal between 25 and 30 K (I_B region) or between 30 and 35 K (I_C region). However, a strong temperature dependent contribution to this elastic constant does arise from the defects which anneal in the temperature

Table 6

The change in the temperature dependence of the resonant frequency of the C' mode introduced by the defects which anneal in three different temperature regions

Temperature (K)	Δf (Hz) Annealing Region 25 to 30 K	Δf (Hz) Annealing Region 30 to 35 K	Δf (Hz) Annealing Region 35 to 45 K
3.6	--	--	--
8		+2	-2
10	+5	-1	-6
13	-6	-3	-9
16	-5	-3	-16
18	-3	+1	-17
20	-9	+1	-22
25	-4	+2	-37
30		-7	-48

interval from 35 to 45 K (stage I_D). In fact, the temperature dependent part of the contribution at 30 K is about half of the zero temperature effect.

This temperature dependence from the I_D defects is not characteristic of a relaxation process. Also, it would be surprising if the polarization and bulk contributions from the individual defects carried a temperature dependence which is so much larger than that of the ideal crystal elastic constants. On the other hand, the large observed temperature dependence could arise from only a small change in the vibrational contribution to the elastic constant from the entire lattice.

The simplest interpretation of a change in the vibrational spectrum is that the Debye characteristic temperature, θ_D, has been shifted as a result of the irradiation. In the Debye approximation,[23] Eq. (9) leads to a $1/\theta_D^5$ temperature dependence of the elastic constants. The required shift of the Debye temperature necessary to produce the observed change in the temperature dependence can therefore be found from the relation:

$$\frac{\Delta\theta_D}{\theta_D} = -\frac{1}{5}\frac{f_d(T_1) - f_d(T_2)}{f_p(T_1) - f_p(T_2)} \quad . \tag{14}$$

Here, $f_d(T)$, is the irradiation produced change in the resonant frequency at temperature T, and $f_p(T)$ is the measured pre-irradiation value of the resonant frequency at temperature T. The present results obtained in the interval from 3.6 to 25 K would then require a fractional change in the Debye temperature of about 4×10^{-3}. However, such a large change in θ_D is not consistent with the observed elastic constant changes. In the Debye approximation, the velocity of sound, v, is assumed constant, and the Debye characteristic temperature is then defined by[54]:

$$\theta_D = \frac{\hbar v}{K}\left(\frac{6\pi^2 N}{V}\right) \quad . \tag{15}$$

Here N is the number of vibrational modes present in a volume, V, of the lattice. Therefore, the change in the Debye characteristic temperature produced by the irradiation is given directly by the change in the velocity of sound:

$$\frac{\Delta\theta_D}{\theta_D} = \frac{\Delta v}{v} . \tag{16}$$

If the observed temperature dependence can be attributed to a shift of the Debye temperature, the relative change of the velocity of the sound wave produced by the I_D defects during irradiation must therefore also be on the order of 4×10^{-3}. The total velocity change which was measured during irradiation of this mode is less than 3×10^{-5}, clearly demonstrating that the radiation induced temperature dependence is far too strong to be explained by a rigid shift of the lattice spectrum.

However, a strong change in the temperature dependence in the low temperature region could be produced by a relatively small change in the vibrational spectrum due to the introduction of new low frequency modes. The computer simulation by Dederichs et al.[11] predicts, in fact, the existence of such modes for the ⟨100⟩-split dumbbell interstitial, with characteristic frequencies of about 1/7 the maximum cut-off value for the ideal lattice. Although Dederichs[43] was concerned with the excitation of these modes by an applied stress, resonant modes can be excited thermally as well.

The result of thermal excitation of resonant modes may be quantitatively analyzed by considering the addition of a number, N, of Einstein oscillators, each of characteristic frequency ω_E, in Eq. (9). The additional contribution to the elastic constants, $\Delta C_{ijk\ell}(T)$, is given by:

$$\Delta C_{ijk\ell}(T) = \frac{\hbar N}{V_0} \frac{\partial^2 \omega_E}{\partial \eta_{ij} \partial \eta_{k\ell}} \left(\tfrac{1}{2} + \frac{1}{e^y - 1}\right)$$

$$- \frac{kNT}{V_0 \omega_E^2} \frac{\partial \omega_E}{\partial \eta_{ij}}\Big)_T \frac{\partial \omega_E}{\partial \eta_{j\ell}}\Big)_T \frac{y^2 e^y}{(e^y - 1)^2} \qquad (17)$$

$$+ \Delta\eta(\tilde{C}^o_{ikj\ell} + \tilde{C}^o_{ijk\ell mm}) \ .$$

Here, $y = \frac{\hbar\omega_E}{kT}$, and $\Delta\eta$ is the change in the vibrational part of the strain. From the equilibrium condition,[23] it is found to be:

$$\Delta\eta = - \frac{\hbar N}{3B}\left(\tfrac{1}{2} + \frac{1}{e^y - 1}\right) \frac{\partial \omega_E}{\partial V}\Big)_T \ . \qquad (18)$$

If we define K_1 and K_2 in the following manner,

$$K_1 = \frac{\hbar N}{V_0} \frac{\partial^2 \omega_E}{\partial \eta_{ij} \partial \eta_{k\ell}} - \hbar N \frac{(C^o_{ijk\ell} + C^o_{ijk\ell mm})}{3B} \frac{\partial \omega_E}{\partial V}\Big)_T$$

and

$$K_2 = \frac{\hbar N}{V_0 \omega_E} \frac{\partial \omega_E}{\partial \eta_{ij}}\Big)_T \frac{\partial \omega_E}{\partial \eta_{k\ell}}\Big)_T$$

we may write the contribution to the elastic constants from the addition of N lattice modes of characteristic frequency ω_E as:

$$\Delta C_{ijk\ell}(T) = K_1\left(\tfrac{1}{2} + \frac{1}{e^y - 1}\right) - K_2 \frac{y e^y}{(e^y - 1)^2} \ . \qquad (19$$

Eq. (19) shows that the introduction of resonant modes into the vibrational spectrum of the lattice produces both a zero-point and temperature dependent effect. It predicts a linear decrease of the elastic constant with temperature for $\hbar\omega_E$ much less than kT, and an exponential temperature dependence for $\hbar\omega_E$ much greater than kT, achieving zero slope at zero degrees Kelvin. In fact, the qualitative temperature dependence of the elastic

constants given by this equation is precisely the behavior exhibited by the I_D defect contribution to the temperature dependence of the C' elastic constant (Table 6).

In order to determine the quantitative agreement between these results and the predicted behavior from defect resonance modes, we may fit the data given in Table 6 to the temperature dependent terms in Eq. (19). In this way, it is possible to obtain an estimate of the frequency associated with the defect which can then be compared to the results of Dederichs et al.[11] The measured contributions from the I_D defects to the temperature dependence of the C' elastic constant are shown in Fig. 24, along with a curve obtained from a least squares fit of the temperature dependent terms in Eq. (19) to this data, using $\omega_E = 5 \times 10^{12}$ Hz. Error bars are given on the figure which represents our own estimate of the experimental uncertainty. Although the curve obtained from the least squares analysis fits the data points extremely well, it is difficult to assign error limits to the resulting values for the three parameters. It is possible to obtain satisfactory fits to the data with frequencies in the range $(1\text{-}9) \times 10^{12}$ Hz. However, we may restrict this range further by requiring reasonable values for the frequency strain derivatives appearing in K_1 and K_2. In the range $\omega_E = (4\text{-}7) \times 10^{12}$ Hz, the magnitude of $\frac{1}{\omega_E} \frac{\partial \omega_E}{\partial \eta_{ij}}$ required for a satisfactory fit varies between approximately 40 and 100. The magnitude of $\frac{1}{\omega_E} \frac{\partial^2 \omega_E}{\partial \eta_{ij} \partial \eta_{k\ell}}$ is a very sensitive function of frequency in this region, ranging from about -10^4 to $+10^4$ and becoming zero at a frequency slightly less than 6×10^{12} Hz. There are no theoretical values with which to compare these numbers, but $\frac{1}{\omega} \frac{\partial \omega}{\partial \eta}$ is approximately 2 for typical lattice modes and $\frac{1}{\omega} \frac{\partial^2 \omega}{\partial \eta^2}$ is on the order of 1-10. The large values obtained from the present results imply that the resonant modes couple very strongly to shear

strains. If we assume the first and second order strain derivatives progressively increase, as with typical lattice modes and higher order elastic constants, the values for these parameters ($\frac{1}{\omega_E}\frac{\partial\omega_E}{\partial\eta_{ij}} \sim 60$ and $\frac{1}{\omega_E}\frac{\partial^2\omega_E}{\partial\eta_{ij}\partial\eta_{k\ell}} \sim 10^3$) required to fit the results for $\omega=5\times10^{12}$ Hz are not unreasonable. However, very large values of the second strain derivative, as much as three orders of magnitude greater than the first derivative are not to be expected. Therefore we believe the frequency of the resonant mode is:

$$\omega_E = 5\times10^{12}\pm30\% \text{ Hz} .$$

This frequency compares very well with the prediction by Dederichs et al.[11] of approximately 6×10^{12} Hz for the ⟨100⟩-split dumbbell interstitial. The magnitude of the zero-point effect calculated from Eq. (19) for this frequency range is only a small fraction of the recovery of the C' elastic constant observed at 3.6 K between annealing pulses of 35 and 45 K.

The limited data obtained with the C_{44} mode permit only the temperature dependence which anneals in the interval between 45 and 60 K (stage I_E) to be separated in the manner discussed above. These results are shown in Fig. 25. Here again, we observe the kind of behavior which is expected if the defects introduce low frequency resonance modes into the vibrational spectrum of the lattice. The fit to Eq. (19) for $\omega_E=5\times10^{12}$ Hz obtained with the C' results has been included in this figure for comparison.

Although these results are also in agreement with the predicted behavior from the introduction of resonance modes, their interpretation is more difficult than in the C' case. As discussed previously, the small amount of annealing which occurs in this temperature range is further

Fig. 24. The change in the temperature dependence of the C' resonant frequency produced by the defects which anneal in the 35 to 45 K temperature range (stage I_D). Since no significant change was observed between 30 and 35 K, both the difference between the 45 and 35 K results and between the 45 and 30 K results are shown. The solid curve represents a least squares fit for $\omega_E=5\times10^{12}$ Hz of the temperature dependence terms in Eq. (19) to the results. The error bars represent our estimate of the experimental uncertainty.

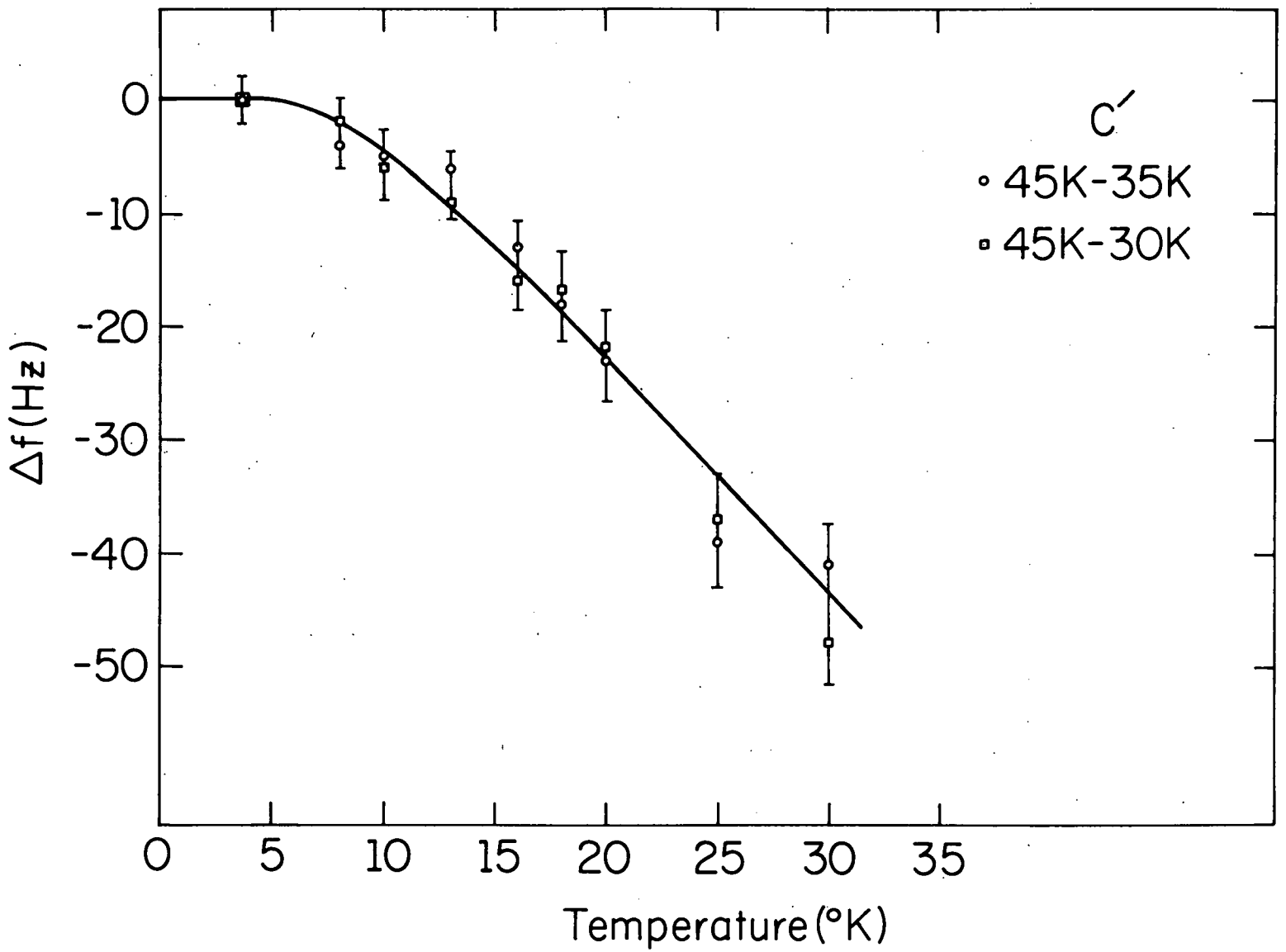
C′
◦ 45K-35K
▫ 45K-30K
Δf(Hz)
0
-10
-20
-30
-40
-50
0
5
10
15
20
25
30
35
Temperature (°K)

Fig. 25. The change in the temperature dependence of the C_{44} resonant frequency from the defects which anneal in the 45 to 60 K temperature range. The solid curve represents the least squares fit of the temperature dependent terms in Eq. (19) obtained with the C' data for $\omega_E = 5 \times 10^{12}$ Hz.

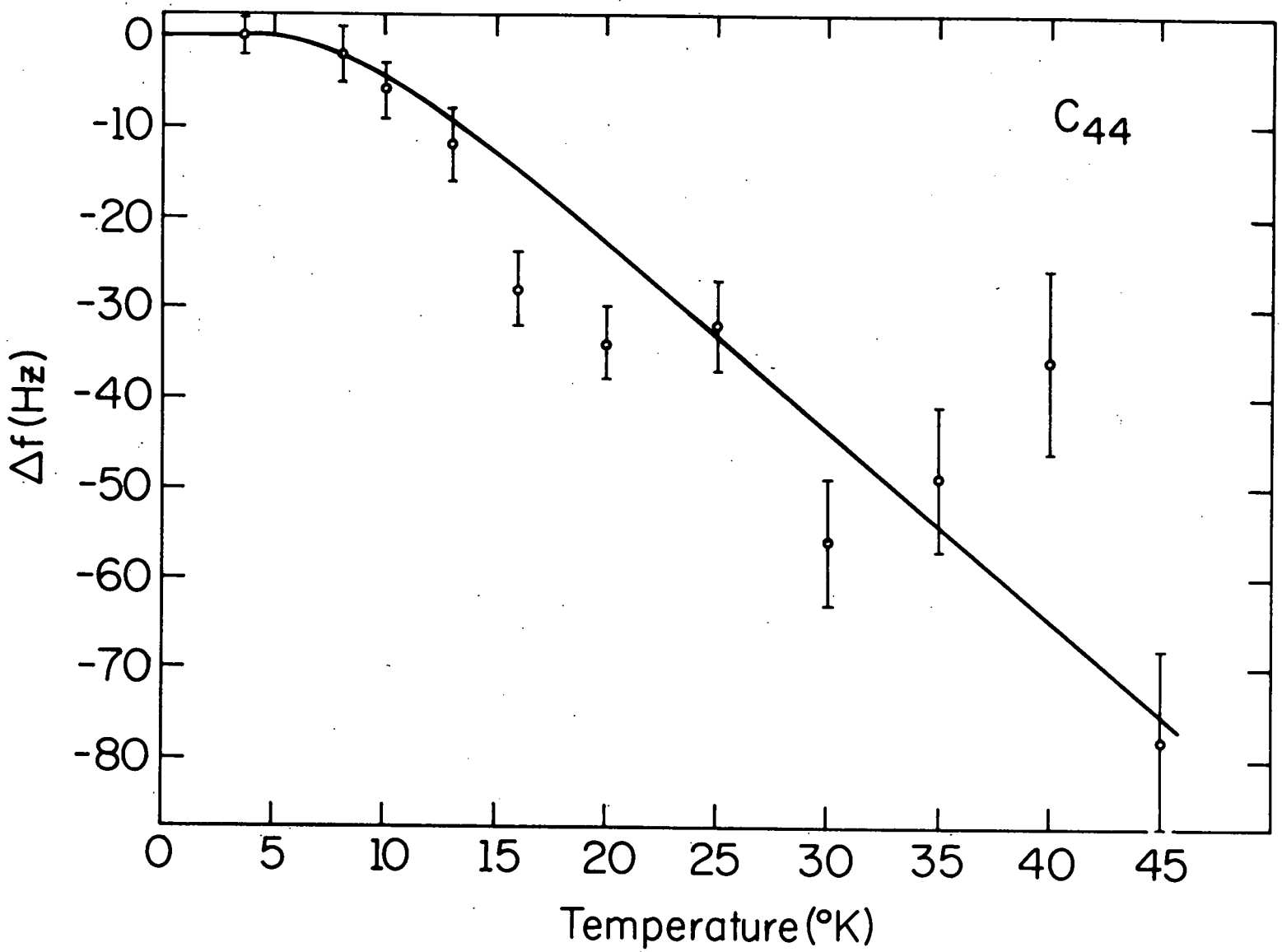
0
-10
-20
-30
-40
-50
-60
-70
-80
Δf (Hz)
C44
0
5
10
15
20
25
30
35
40
45
Temperature (°K)

complicated by the clustering and trapping of defects during the long-range interstitial migration. Hence the change in the temperature dependence which occurs in this interval may be significantly affected by the new types of defects which are created. Therefore, the important question of whether the frequency found from the C_{44} data is the same as the frequency observed in the C' mode cannot be answered on the basis of the present results.

The preceding discussion indicates that low frequency resonance modes cause a significant change in the normal temperature dependence of the elastic constants of irradiated crystals. The question then arises as to the magnitude of similar contributions to the temperature dependence of other physical properties. For example, the vibrational energy associated with a defect resonance mode should contribute to the stored energy of an irradiated solid. This energy (approximately 4×10^{-3} eV at 35 K for a frequency of 5×10^{12} Hz) is very small in relation to the value of about 5 eV for the formation energy of a frenkel pair, and therefore would not be discernible in a measurement of the stored energy released during annealing. However, this effect would also contribute to the heat capacity of the irradiated solid at temperatures below the annealing range of the defects which possess the resonance modes. The magnitude of this contribution may be estimated by considering the change in the heat capacity at constant volume, ΔC_V, produced by N defects each with one resonance mode of frequency ω_E[23]:

$$\Delta C_V = \frac{N}{k} \left(\frac{\hbar\omega_E}{T}\right)^2 \frac{e^{\frac{\hbar\omega_E}{kT}}}{\left(e^{\frac{\hbar\omega_E}{kT}} - 1\right)^2} \quad . \tag{20}$$

The relative contribution from a resonance mode at any given temperature to

the specific heat is therefore determined only by its characteristic frequency. This calculation gives a maximum contribution at a temperature near 9 K. At this temperature, it gives a change in the total heat capacity of copper of 2.2×10^{-4} J/mole-deg (approximately 0.5% of the total specific heat at this temperature) for a resonance frequency of 5×10^{12} Hz and an atomic fraction of contributing defects of 10^{-4}. For frequencies of 4×10^{12} Hz and 6×10^{12} Hz, and the same concentration of defects, the change in the total specific heat at this temperature would be approximately 0.8% and 0.3% respectively. Changes in the heat capacity of this magnitude can be easily measured,[55] so that a measurement of the irradiation produced change in the heat capacity at low temperatures should permit an accurate determination of the frequency of the resonance mode.

The presence of these modes should also change the temperature dependence of the lattice thermal expansion. The magnitude of this contribution is given by Eq. (18). However, since the value of $\frac{\partial \omega_E}{\partial V}$ is unknown, no estimate can be given.

The temperature dependence of the electrical resistivity (deviations from Matthiessen's rule) should likewise be altered by the introduction of defect vibrational modes. In fact, the large resistivity effects observed by Magnuson, Palmer and Koehler,[1] and which they interpreted as a large shift in the Debye characteristic temperature, are probably a consequence of the creation of resonance modes characteristic of stage I defects. However, the effect on the resistivity temperature dependence is difficult to analyze quantitatively, and no estimate will be given.

In conclusion, the present results indicate that resonance modes should significantly change the temperature dependence of

a number of physical properties. Since changes in elastic constants can be measured very accurately at low temperatures, and because their temperature dependence can be easily related to resonance mode effects, the measurement of temperature dependent effects of stage I defects on the elastic constants provides a particularly convenient means for investigating the properties of resonance modes. A more detailed experiment especially designed for measuring irradiation produced changes in the temperature dependence of the elastic constants in the range from 3 to 25 K seems quite promising.

V. SUMMARY

This thesis has been concerned with the changes introduced in the elastic constants of copper from the production of point defects by low temperature irradiation. Four different mechanisms through which point defects may alter the elastic constants of a metal were known prior to completion of the present experiments: (1) bulk and (2) polarization effects; (3) relaxation processes and (4) dislocation pinning. Another mechanism, (5) the excitation of defect resonance modes, has been proposed to explain certain of the results obtained in the present study.

By far the largest potential contribution comes from the pinning of dislocation segments, and therefore must first be eliminated if the other effects are to be studied. This was accomplished in the present case by a room temperature fast neutron irradiation of low-dislocation-density samples. There is considerable evidence to show this procedure was effective in saturating out pinning effects: The marked linearity of the measured changes in the elastic constants and attenuation during irradiation; the agreement between two different C_{11} and C_{44} irradiation runs; the magnitude of the recovery of the elastic constants during annealing, which was always less than the measured change during irradiation; the good agreement in the annealing behavior of the two different C_{44} runs; the increase in the attenuation which was always found during annealing, as well as the close agreement between the recovery of the resistivity and attenuation changes produced by the low temperature irradiation with each other, and with the theoretical estimates; the close agreement which was found between the pre-irradiation measurements of the temperature dependence of the elastic constants and the perfect crystal calculations of Garber and Granato[23]; and the agreement

between the value of the relaxation shape factor, $|\lambda_1-\lambda_2|$, determined on the basis of the present results and that calculated from the Nielsen and Townsend[9] study.

Several features of the present experiments were essential in extracting accurate information about particular defects from the total irradiation produced changes in the elastic constants, and in separating the contributions from different kinds of effects. (A) The present measurements were made on a complete set (C_{11}, C_{44} and C') of independent cubic elastic constants. This allows calculation of the changes to be expected in any cubic elastic constant (bulk modulus, Young's modulus, etc.). Knowledge of these changes is useful in the comparison of different experiments, as well as in the separation of various effects. In addition, measurements of the behavior of a complete set of constants is helpful in determining the symmetry of certain of the contributing defects. (B) The high degree of sensitivity which was achieved by use of the pulse-echo superposition technique, permitted a quantitative study of the annealing behavior of the irradiation produced changes. This in turn allowed investigation of the contributions from particular stage I defects. (C) The simultaneous measurement of the resistivity and attenuation gave an accurate measurement of the concentration of irradiation induced defects. Finally, (D) the measurement of the change in the temperature dependence of the elastic constants produced by the irradiation, and its annealing, allowed the relaxation and resonance mode effects to be studied.

The present measurements of the changes in the elastic constants during irradiation (Table 1) lie intermediate in the range of previously reported values, and show that the wide range of reported values cannot be understood in terms of the different elastic constants which were measured.

It was found that the contributions from different stage I defects to a particular elastic constant were not the same, and also, the magnitude of the effect from a given defect was found to vary among different elastic constants. The results obtained here can be understood in terms of four mechanisms.

1. The bulk effect is a result of the change in number and strength of inter-atomic bonds caused by the creation of isolated vacancies and interstitials. Based on the results obtained for the change in the bulk modulus during annealing through stage I, this effect is so small $\left(\left|\frac{d\ell nB}{d\gamma}\right)_{\text{stage I}}\right| < 1\right)$ relative to the other contributions, that not even its sign is known. This indication of a small effect is in agreement with the range of reported theoretical estimates (-10 to +10).

2. Polarizability effects occur for defects whose atoms are not at perfect crystal lattice sites. In this case, an internal strain can be produced by the application of an applied stress, and this additional strain causes a decrease in the measured elastic constant. This effect may be quite large, and the variation in its magnitude among different elastic constants depends upon the symmetry of the defect. The results obtained at 3.6 K for the recovery of the three elastic constants and resistivity during stage I_D are qualitatively in agreement with the calculation by Dederichs[43] of the polarizability of the ⟨100⟩-split dumbbell interstitial.

3. Relaxation involves the thermally activated, stress-induced ordering of preferential defect orientations, and therefore is a temperature dependent effect. The relaxation process previously reported by Nielsen and Townsend[9] has been observed. By combining the present results with those of NT, values have been obtained for the attempt frequency and energy of activation which

are in good agreement with those reported solely on the basis of the NT results. We have attributed this relaxation to the I_C defect, and a model of this defect (Fig. 23) has been proposed. No other relaxation of stage I defects has been observed. In particular, no relaxation process was found to contribute to any of the modulus changes measured at 3.6 K.

4. The excitation of defect resonance modes changes the vibrational spectrum of the lattice. This in turn introduces both a zero-point and temperature dependent change in the elastic modulus. The results obtained for the change in the temperature dependence of the C' elastic constant induced by the I_D defects are in good agreement with the expected behavior from defect resonance modes. Based on a simplifying assumption, the frequency is believed to be:

$$\omega = 5 \times 10^{12} \pm 30\% \text{ Hz} .$$

This frequency is in reasonable agreement with the value of approximately 6×10^{12} Hz obtained by Dederichs et al.[11] by a computer simulation of a ⟨100⟩-split interstitial in a copper lattice. The results for the temperature dependent change in the C_{44} elastic constant introduced by the I_E defects (Fig. 25) is also consistent with the expected behavior from defect resonance modes. However, the interpretation of the effect is more difficult in this annealing range, and it is not possible to say from the present results whether or not the frequency obtained from these results is the same as that from the I_D defects.

Based on the value of the frequency obtained here, the excitation of resonance modes should also contribute significantly to the temperature dependence of other physical properties. In particular, low temperature elastic constant and heat capacity measurements should serve as tools with which to investigate this phenomenon.

In conclusion, we turn to one of the original questions posed in the introduction: Why is there such a wide range in the values reported by different investigators for the magnitude of the change in elastic modulus as a function of Frenkel pair damage? The present results indicate that some difference is to be expected between measurements on different elastic constants, and with different types of irradiation, but the large differences in reported magnitudes cannot be explained by these effects. However, some of the other results obtained here are helpful in explaining most of the apparent discrepancies.

A brief description of each of the reported measurements of irradiation induced changes in the elastic modulus is given in Tables 7 and 8. The first table (7) is included for the sake of completeness, and lists the studies on materials other than copper. No comparison of these results will be attempted. The experiments involving copper are shown in Table 8.

Two of these studies, by Dieckamp and Sosin,[13] and Roth and Naundorf,[15] were conducted at liquid nitrogen temperatures, and both report large effects. These large effects may be understood in terms of the strong change in the temperature dependence of the elastic constants which was observed after stage I annealing.

The remaining measurements were all at or near liquid helium temperatures. The two investigations which represent the extremes of all the reported values, Thompson et al.[12] and Konig et al.[14] are not consistent with the present results or with any other similar measurement. The failure of Thompson et al. to observe any effect is the most difficult to understand, especially since the experiment by Wenzel et al.[17] is so similar in nature. Possibly, some cancellation due to dislocation pinning effects

occurred during the measurement. The difficulties in the Konig et al. experiment have been discussed elsewhere, in terms of both the inhomogeneity of damage in their sample,[9] as well as the uncertainty in the assumed frenkel pair production rate.[56]

Wenzel et al.[17] report a value of -39 using reactor irradiation, which is about twice as large as would be expected on the basis of the present results if the type of damage was the same. However, the damage introduced by reactor irradiation is more complex than that created by thermal neutrons, and is characterized by large depletion zones. It is quite possible that these zones may contribute significantly to the measured modulus changes, and thus account for the larger observed value. In fact, the annealing studies by Ehrensperger,[10] show that only about 20% of the observed shear modulus change in copper produced by fast neutron irradiation anneals in stage I. This indicates that studies of fast neutron induced changes in the elastic moduli of copper are primarily measurements of other than stage I defects.

The findings of Okuda and Nakanii,[16] which give only an upper limit on the magnitude of the effect (-80), are consistent with the present findings.

Excellent agreement is obtained with the Townsend et al. and Nielsen and Townsend results[9] of -13 ± 3. Excellent agreement was also obtained previously with their values for the parameters associated with the relaxation process. Since deuteron and thermal neutron damage is quite similar in nature, this high degree of agreement should be expected.

Table 7
A brief description of the reported measurements of irradiation induced changes in the elastic modulus of various materials other than copper

	$\frac{d \ell nC}{d\gamma}$	Material	Radiation Type	Radiation Temperature (K)	Measurement Temperature (K)	Simultaneous Resistivity	Measurement Frequency (Hz)
Likhter and Kikoin[57]	No effect on bulk modulus	Mg Al	Reactor Neutrons	300	300	No	--
Muss and Townsend[58]	-0.44	W	13.7 Mev D	300	300	No	10^3-10^4
Gerlich et al.[18]	Small	LiF	Reactor Neutrons	300	300	No	10^7
Folweiler and Brontzen[59]	-10	Al	Quench (only vacancies)	Quench from 800	300	No	10^5
DiCarlo and Townsend[60]	-(.2-1)	W	13 Mev D	78-90	78	No	10^3-10^4
Hillairet et al.[61]	Large	Mg	Reactor Neutrons	80	80	No	--
DiCarlo et al.[62]	-11	W	2.5 Mev Electrons	$\leq$ 20	$\leq$ 20	Yes	600
Chountas et al.[63]	-39±9	Ag	Reactor Neutrons	25	10	Yes	44 140
Soulie et al.[64]	-70	Ni	2 Mev Electrons	11-21	11-21	Yes	350

Table 8
A brief description of the reported measurements of irradiation induced changes in the elastic modulus of copper

	$\frac{d\ell nC}{d\gamma}$	Material	Radiation Type	Radiation Temperature (K)	Measurement Temperature (K)	Simultaneous Resistivity	Measurement Frequency (Hz)
Present Experiment	C_{11} - 4.8 C_{44} -15.8 C' -18.1	Cu	Thermal Neutrons	4	3.6	Yes	10^7
Dieckamp and Sosin[13]	-140±60	Cu	1 Mev Electrons	78-206 (gradient)	78	No	500
Roth and Naundorf[15]	- 75±20	Cu	3 Mev Electrons	120	78	Yes	2.5×10^3
Thompson et al.[12]	none (< 1)	Cu	Reactor Neutrons	21	21	No	10^4
Konig et al.[14]	-130	Cu	5.3 Mev α	30	30	No	10^2
Okuda and Nakanii	< -80	Cu	Reactor Neutrons	< 15	4	No	4×10^{12}
Wenzl et al.[17]	-39 -47 -67	Cu Al Pt	Reactor Neutrons	4	4	Yes	50-300
Nielsen and Townsend, Townsend et al.[9]	-13±3	Cu W	10 Mev P	< 15	4.2	No	$5\text{-}20\times10^2$

REFERENCES

1. G. D. Magnuson, W. Palmer, and J. S. Koehler, Phys. Rev. 109, 1990 (1958).

2. J. W. Corbett, R. B. Smith, and R. M. Walker, Phys. Rev. 114, 1452 (1959).

3. J. W. Corbett, R. B. Smith, and R. M. Walker, Phys. Rev. 114, 1460 (1959).

4. G. J. Dienes, Phys. Rev. 86, 228 (1952); G. J. Dienes, Phys. Rev. 87, 666 (1952).

5. C. Zener, Acta Cryst. 2, 163 (1949).

6. F. R. N. Nabarro, Phys. Rev. 87, 665 (1952).

7. J. Melngalis, Phys. Stat. Sol. 16, 247 (1966).

8. R. De Baptist, Internal Friction of Structural Defects in Crystalline Solids, North-Holland Publishing Company, Amsterdam and London (1972).

9. R. L. Nielsen and J. R. Townsend, Phys. Rev. Lett. 21, 1749 (1968); J. R. Townsend, J. A. DiCarlo, R. L. Nielsen, and D. Stabell, Acta. Met. 17, 425 (1969).

10. K. Ehrensperger, Diplomarbeit, Technische Hochschule, Munchen (1969).

11. P. H. Dederichs, C. Lehmann and A. Scholz, Phys. Rev. Lett. 31, 1130 (1973).

12. D. O. Thompson, T. H. Blewitt, and D. K. Holmes, J. Appl. Phys. 28, 742 (1957).

13. H. Dieckamp and A. Sosin, J. Appl. Phys. 27, 1416 (1956).

14. D. Konig, J. Volkl, and W. Schilling, Phys. Stat. Sol. 7, 591 (1964).

15. G. Roth and V. Naundorf, Jül. Conf. 2 (Vol. I), 364 (1968).

16. S. Okuda and T. Nakani , Radiation Damage in Reactor Materials, International Atomic Energy Agency, Vienna (1969).

17. K. Ehrensperger, H. Wenzl, F. Kerscher, V. Fischer and K. Papathanassopoulos, Z. Naturforsch. 26, 489 (1971).

18. D. Gerlich, J. Holder, and A. Granato, Phys. Rev. 181, 1220 (1969).

19. A. C. Damask and G. J. Dienes, Point Defects in Metals, Gordon and Breach Science Publishers, New York and London (1963).

20. R. R. Coltman, Jr., C. E. Klabunde, D. L. McDonald, and J. K. Redman, J. Appl. Phys. 33, 3509 (1962).

21. K. S. Krishman and S. K. Roy, Proc. Roy. Soc. (London) 210, 481 (1952).

22. F. W. Young, Jr. and J. R. Savage, J. Appl. Phys. 35, 1917 (1964).

23. J. Garber and A. V. Granato, private communication.

24. F. W. Young, Jr. and T. R. Wilson, Rev. Sci. Instr. 32, 559 (1961).

25. J. W. Mitchell, J. C. Chevrier, B. J. Hockey, and J. P. Monaghan, Jr., Can. J. Phys. 45, 453 (1967).

26. J. S. Ahearn, Jr., J. P. Monaghan, Jr., and J. W. Mitchell, Rev. Sci. Instr. 41, 1853 (1970).

27. T. Ochs, J. Phys. E: Sci. Instrum. 1, 1122 (1968).

28. R. R. Coltman, T. H. Blewitt, and T. S. Noggle, Rev. Sci. Instr. 28, 357 (1957).

29. R. R. Coltman, C. E. Klabunde, and J. K. Redman, Phys. Rev. 156, 715 (1967).

30. J. Holder, Rev. Sci. Instr. 41, 1355 (1970).

31. D. Read and J. Holder, Rev. Sci. Instr. 43, 933 (1972).

32. H. J. McSkimin and P. Andreatch, Jr., J. Acoust. Soc. Am. 41, 1052 (1967).

33. H. G. Cooper, J. S. Koehler, and J. W. Marx, Phys. Rev. 97, 599 (1955).

34. R. Vook and C. Wert, Phys. Rev. 109, 1529 (1958).

35. R. O. Simmons and R. W. Balluffi, Phys. Rev. 109, 1142 (1958).

36. R. R. Coltman, Jr., C. E. Klabunde, J. K. Redman and A. L. Southern, Rad. Effects 16, 25 (1972).

37. W. Köster and W. Rauscher, Z. Metallk. 39, 111 (1948).

38. W. Schilling, Private communication (1973).

39. G. A. Alers, in Physical Acoustics, edited by W. P. Mason (Academic Press, Inc., New York, 1966), Vol. IVA, p. 277.

40. T. G. Nilan and A. V. Granato, Phys. Rev. 137, A1233 (1965).

41. A. V. Granato and T. G. Nilan, Phys. Rev. 137, A1250 (1965).

42. C. L. Snead, F. W. Wiffen and J. W. Kauffman, Phys. Rev. 164, 900 (1967).

43. P. H. Dederichs, private communication (1973).

44. M. Pistorius and W. Ludwig, Jül. Conf. 2 (Vol. 2) 558 (1969).

45. A. B. Pippard, Phil. Mag. 46, 1104 (1955).

46. W. P. Mason, in Physical Acoustics, edited by W. P. Mason (Academic Press, Inc., New York, 1966) Vol. IVA, p. 299.

47. A. S. Nowick and B. S. Berry, Anelastic Relaxation in Crystalline Solids, Academic Press, Inc., New York (1972).

48. W. Schilling, in Vacancies and Interstitials in Metals, edited by A. Seeger, D. Schumacher, W. Schilling, and J. Diehl, North-Holland Publ. Company, 1970, p. 264.

49. H. B. Huntington, Phys. Rev. 91, 1092 (1953).

50. R. A. Johnson and E. Brown, Phys. Rev. 127, 446 (1962).

51. A. Seeger, E. Mann and R. V. Jan, J. Phys. Chem. Solids 23, 639 (1962).

52. J. B. Gibson, A. N. Goland, M. Milgram and G. H. Vineyard, Phys. Rev. 120, 1229 (1960).

53. P. Peretto, J. L. Oddou, C. Minier-Cassayre, D. Dautrepp and P. Moser, Phys. Stat. Sol. 16, 281 (1966).

54. C. Kittel, Introduction to Solid State Physics, Third Edition, John Wiley and Sons, Inc. (1966).

55. G. Ahlers, Rev. Sci. Instr. 37, 477 (1966).

56. H. Wenzl, in Vacancies and Interstitials in Metals, edited by A. Seeger, D. Schumacher, W. Schilling, and J. Diehl, North-Holland Publ. Company, 1970, p. 391.

57. A. I. Likhter and A. I. Kikoin, J. Exptl. and Theoret. Phys. (U.S.S.R.) 32, 945 (1957).

58. D. R. Muss and J. R. Townsend, J. Appl. Phys. 33, 1804 (1962).

59. R. C. Folweiler and F. R. Brotzen, Acta. Met. 7, 716 (1959).

60. J. A. DiCarlo and J. R. Townsend, Acta. Met. 14, 1715 (1966).

61. J. Hillairet, E. Bonjour and J. P. Poirier, Journal de Physique 7, C2-31 (1971).

62. J. A. DiCarlo, C. L. Snead and A. N. Goland, Bull. Am. Phys. Soc. series II, 13, 381 (1968).

63. K. Chountas, W. Donitz, K. Papathanassopoulos and G. Vogl, Phys. Stat. Sol. 53, 219 (1972).

64. J. C. Soulie, J. Lauzier and C. Minier, Rad. Effects 19, 63 (1973).

VITA

Lynn Eduard Rehn was [redacted] He received his primary and secondary education at Harbor Beach Community School, Harbor Beach, Michigan. He attended Albion College, Albion, Michigan, on an Edison Scholarship and received his B.A. degree in Physics and Math (with honors) in June, 1967. He entered the Graduate College, University of Illinois in September, 1967, and received an M.S. degree in Physics in February, 1969. He is a member of the American Physical Society.